Antitumor activity of quinazolinone alkaloids inspired by marine natural products

Solida Long [1], Diana I. S. P. Resende [1,2], Anake Kijjoa [2,3], Artur M. S. Silva [4], André Pina [5,6,7], Tamara Fernández-Marcelo [5,6], M. Helena Vasconcelos [5,6,8], Emília Sousa [1,2,*], and **Madalena M. M. Pinto [1,2]**

[1] Laboratório de Química Orgânica e Farmacêutica, Departamento de Ciências Químicas, Faculdade de Farmácia, Universidade do Porto, Rua de Jorge Viterbo Ferreira, 228, 4050-313 Porto, Portugal. E-mail: up201502099@ff.up.pt (S.L.), madalena@ff.up.pt (M.M.M.P).

[2] Interdisciplinary Centre of Marine and Environmental Research (CIIMAR), Terminal de Cruzeiros do Porto de Lexões, Av. General Norton de Matos s/n, 4450-208, Matosinhos, Portugal. E-mail: dresende@ff.up.pt.

[3] *ICBAS* - Instituto de Ciências Biomédicas Abel Salazar, Universidade do Porto, Rua de Jorge Viterbo Ferreira, 228, 4050-313 Porto, Portugal. E-mail: ankijjoa@icbas.up.pt.

[4] QOPNA, Department of Chemistry, University of Aveiro, 3810-193 Aveiro, Portugal. E-mail: artur.silva@ua.pt (A.S.)

[5] i3S - Instituto de Investigação e Inovação em Saúde, Universidade do Porto, Portugal. E-mail: andre.fig.pina@gmail.com (A.P.), tmarcelo@ipatimup.pt (T.M.), hvasconcelos@ipatimup.pt (H.V.)

[6] Cancer Drug Resistance Group, IPATIMUP - Institute of Molecular Pathology and Immunology of the University of Porto, Portugal;

[7] FCUP - Faculty of Sciences of the University of Porto, Portugal;

[8] Laboratório de Microbiologia, Departamento de Ciências Biológicas, Faculdade de Farmácia, Universidade do Porto, Portugal.

* Correspondence: esousa@ff.up.pt; Tel.: +351-2-2042-8689

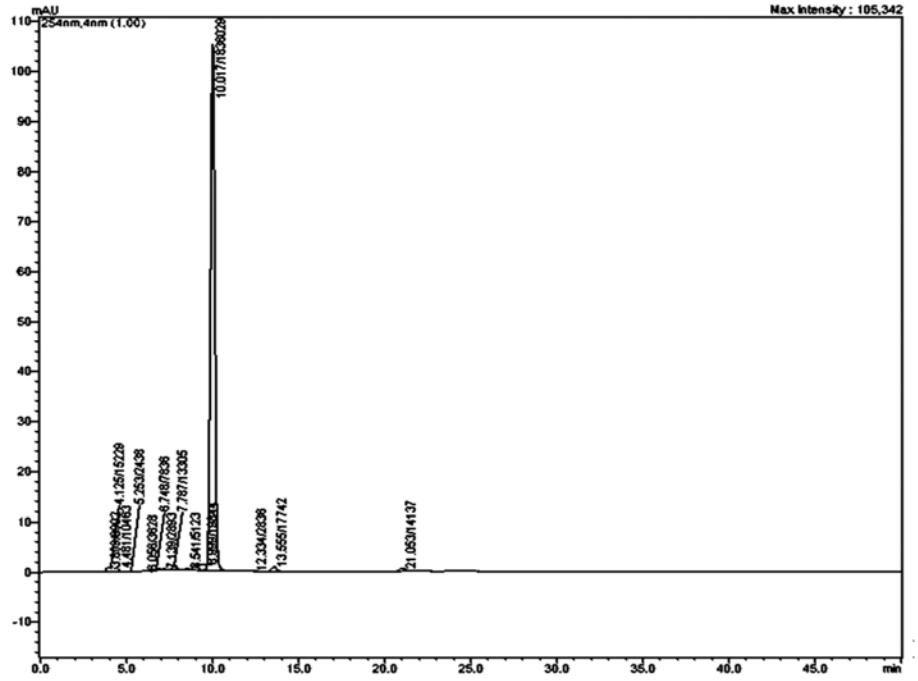

Figure S1. Peak purity analysis of compound **4a** using RP-HPLC with diode array detector (DAD), C18 column (Kimetex®, 2.6 EV0 C18 100 Å, 150 × 4.6 mm); mobile phase: methanol: water (60:40); flowrate: 1 mL/min.

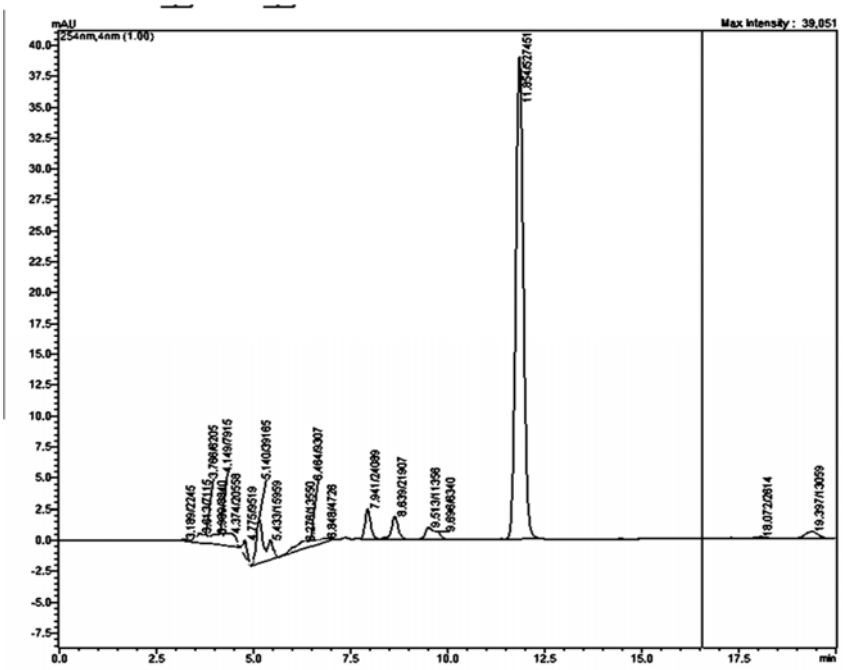

Figure S2. Peak purity analysis of compound **4b** using RP-HPLC with diode array detector (DAD), C18 column (Kimetex®, 2.6 EV0 C18 100 Å, 150 × 4.6 mm); mobile phase: methanol: water (60:40); flowrate: 0.5 mL/min.

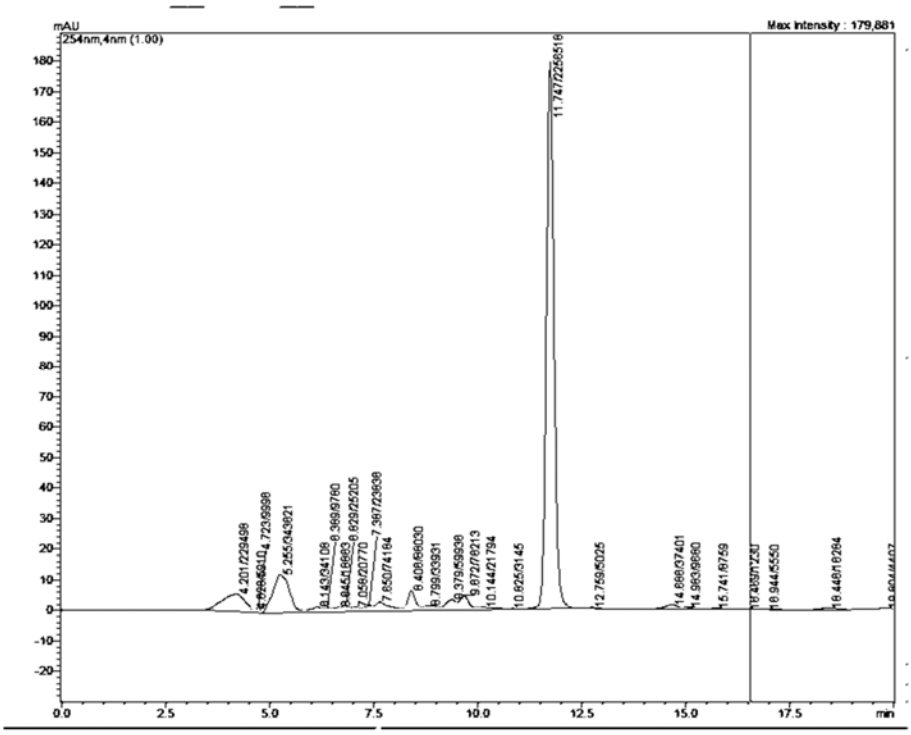

Figure S3. Peak purity analysis of compound **4c** using RP-HPLC with diode array detector (DAD), C18 column (Kimetex®, 2.6 EV0 C18 100 Å, 150 × 4.6 mm); mobile phase: methanol: water (60:40); flowrate: 0.5 mL/min.

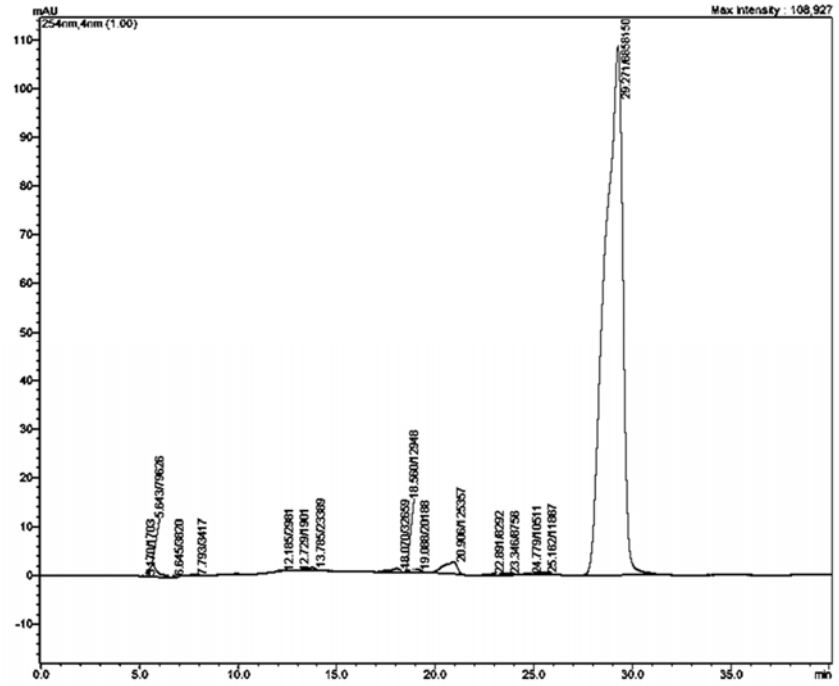

Figure S4. Peak purity analysis of compound **4d** using RP-HPLC with diode array detector (DAD), C18 column (Kimetex®, 2.6 EV0 C18 100 Å, 150 × 4.6 mm); mobile phase: methanol: water (60:40); flowrate: 0.5 mL/min.

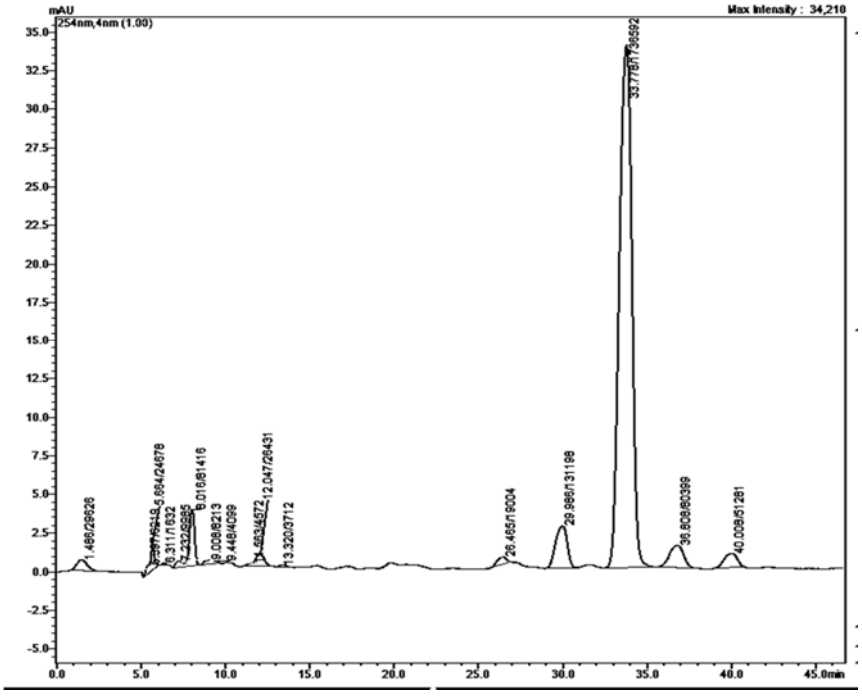

Figure S5. Peak purity analysis of compound **5a** using RP-HPLC with diode array detector (DAD), C18 column (Kimetex®, 2.6 EV0 C18 100 Å, 150 × 4.6 mm); mobile phase: methanol: water (60:40); flowrate: 0.5mL/min.

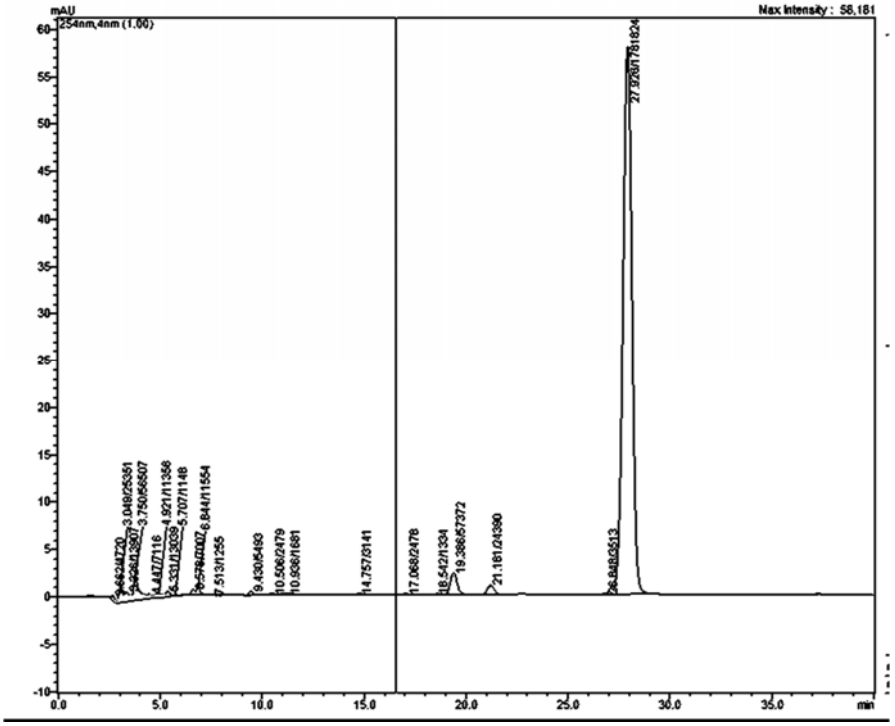

Figure S6. Peak purity analysis of compound **5b** using RP-HPLC with diode array detector (DAD), C18 column (Kimetex®, 2.6 EV0 C18 100 Å, 150 × 4.6 mm); mobile phase: methanol: water (60:40); flowrate: 0.5 mL/min.

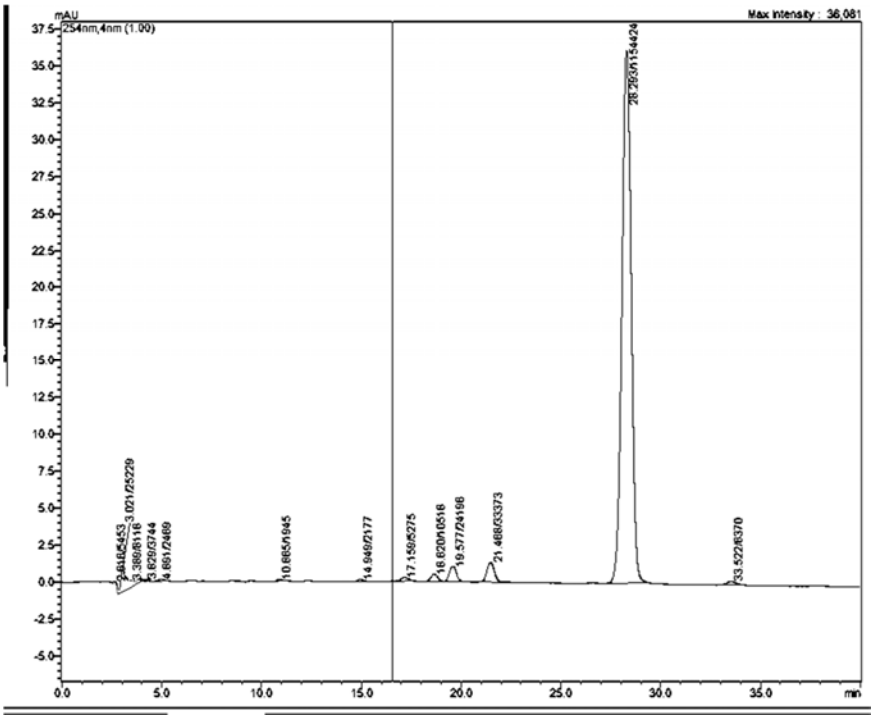

Figure S7. Peak purity analysis of compound **5c** using RP-HPLC with diode array detector (DAD), C18 column (Kimetex®, 2.6 EV0 C18 100 Å, 150 × 4.6 mm); mobile phase: methanol: water (60:40); flowrate: 0.5 mL/min.

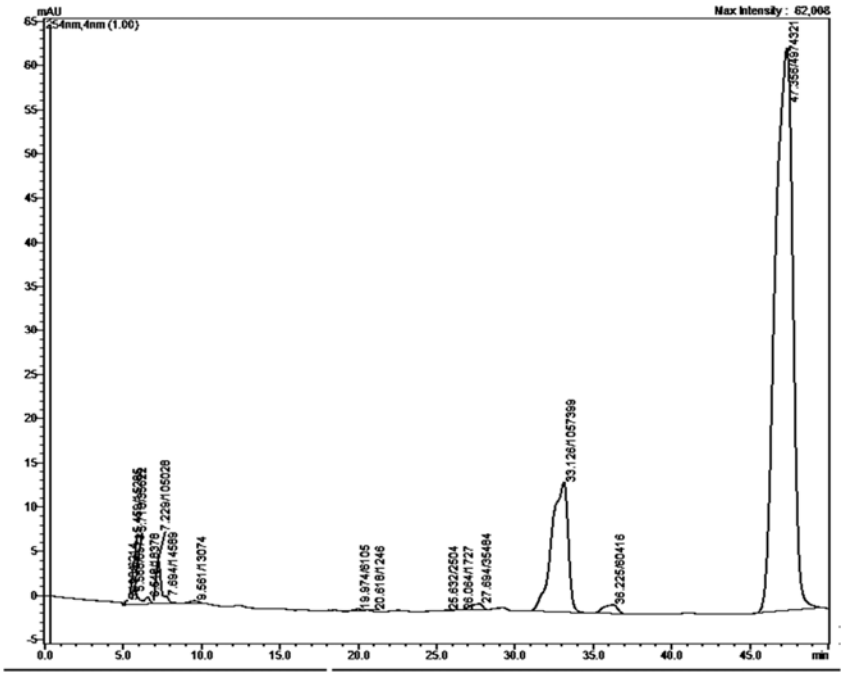

Figure S8. Peak purity analysis of compound **5d** using RP-HPLC with diode array detector (DAD), C18 column (Kimetex®, 2.6 EV0 C18 100 Å, 150 × 4.6 mm); mobile phase: methanol: water (60:40); flowrate: 0.5 mL/min.

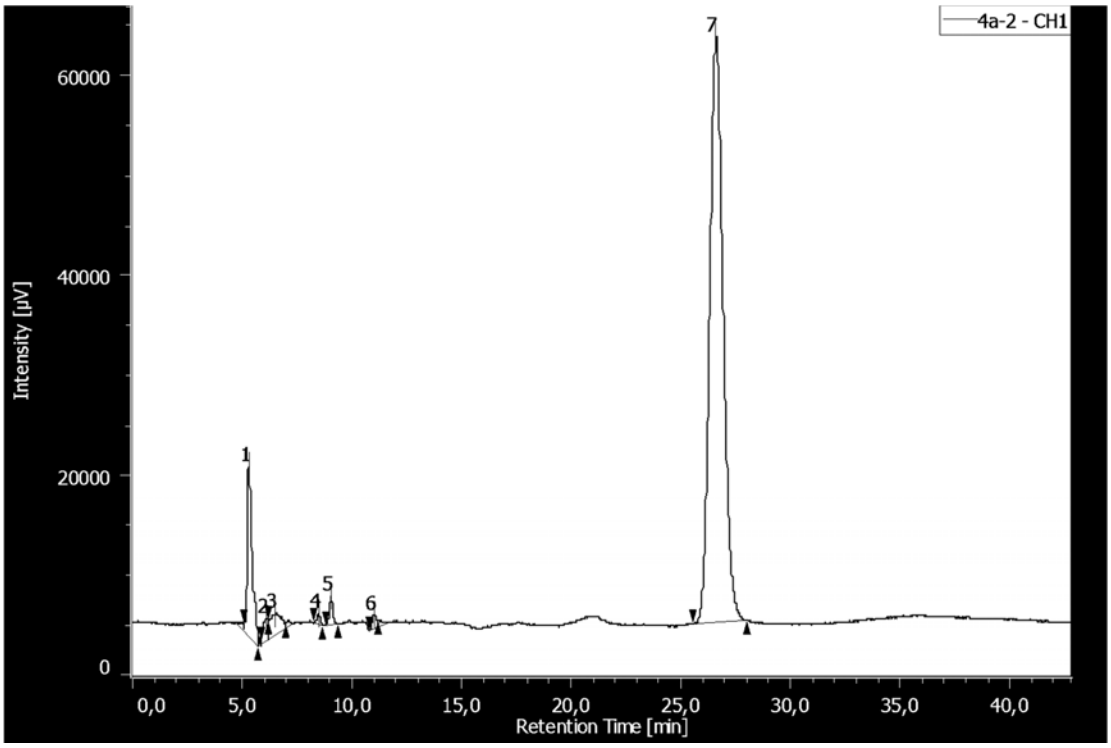

Figure S9. Chiral analysis of (1*S*,4*S*)-4-(1*H*-indol-3-ylmethyl)-1-isopropyl-2*H*-pyrazino[2,1-*b*]quinazolin-3,6-(1*H*, 4*H*)-dione (**4a**). Column: Lux® 5 µm Amylose-1, 250 × 4.6 mm; UV-detection: 254 nm; mobile phase: hexane:ethanol (80:20); flow rate: 0.5 mL/min.

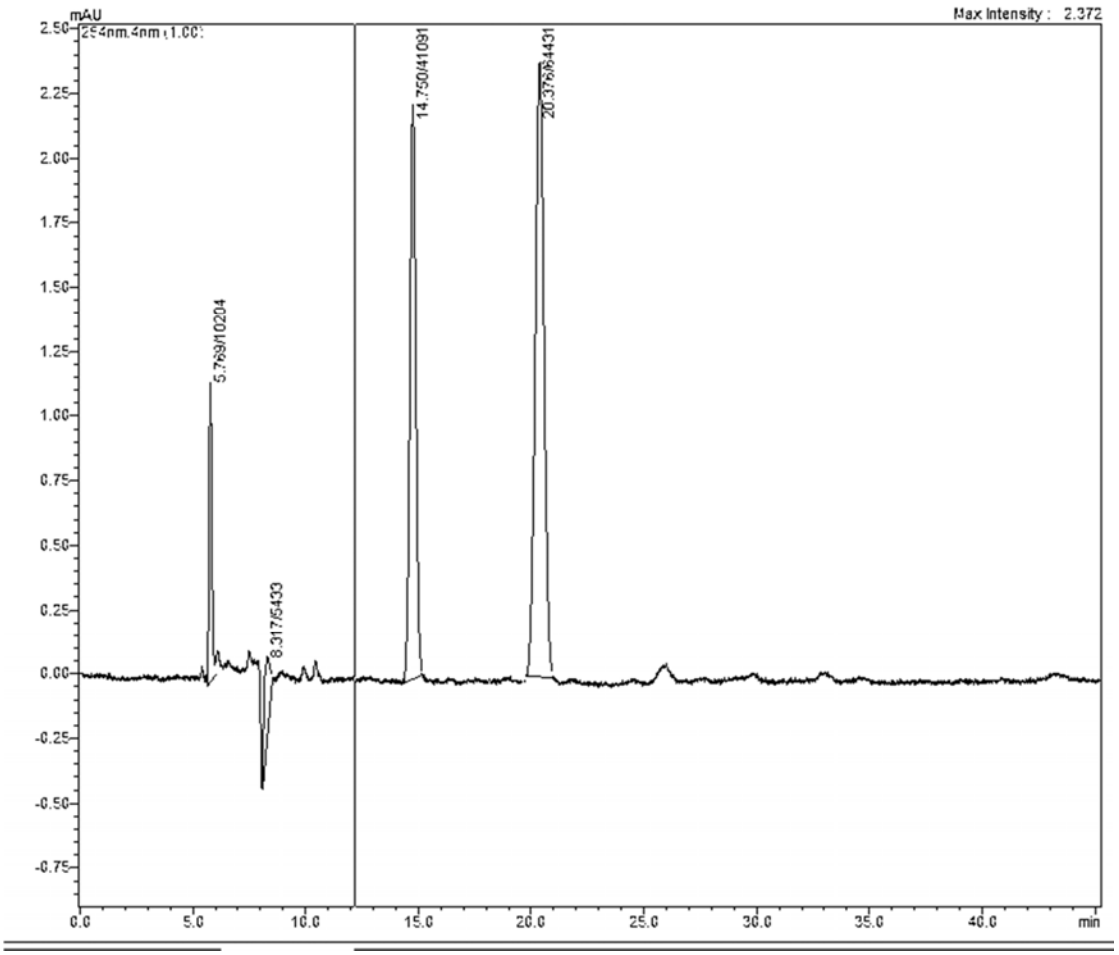

Figure S10. Chiral analysis of (1*S*,4*R*)-4-(1*H*-indol-3-ylmethyl)-1-isopropyl-2*H*-pyrazino[2,1-*b*]quinazolin-3,6-(1*H*, 4*H*)-dione (**4b**). Column: Lux® 5 µm Amylose-1, 250 × 4.6 mm; UV-detection: 254 nm; mobile phase: hexane:ethanol (80:20); flow rate: 0.5 mL/min.

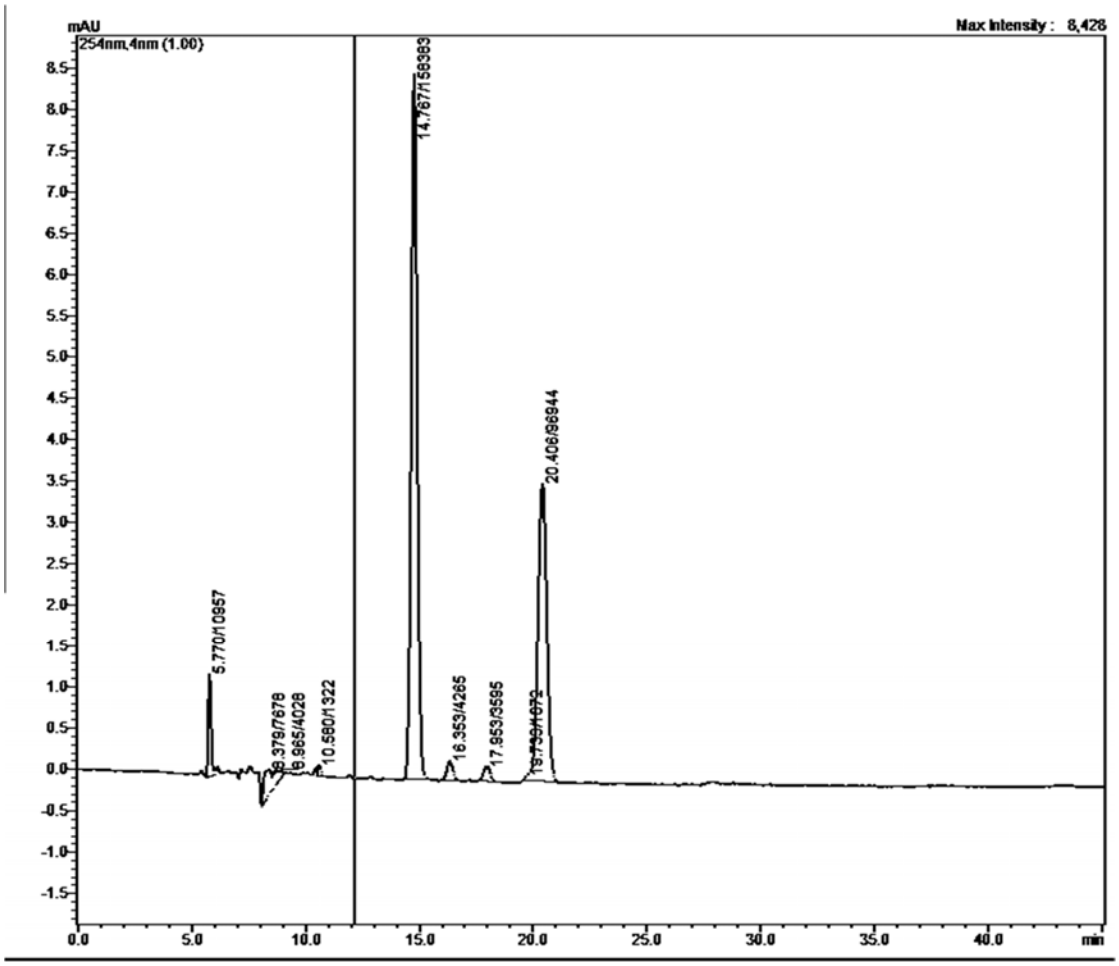

Figure S11. Chiral analysis of (1*R*,4*S*)-4-(1*H*-indol-3-ylmethyl)-1-isopropyl-2*H*-pyrazino[2,1-*b*]quinazolin-3,6-(1*H*, 4*H*)-dione (**4c**). Column: Lux® 5 µm Amylose-1, 250 × 4.6 mm; UV-detection: 254 nm; mobile phase: hexane:ethanol (80:20); flow rate: 0.5 mL/min.

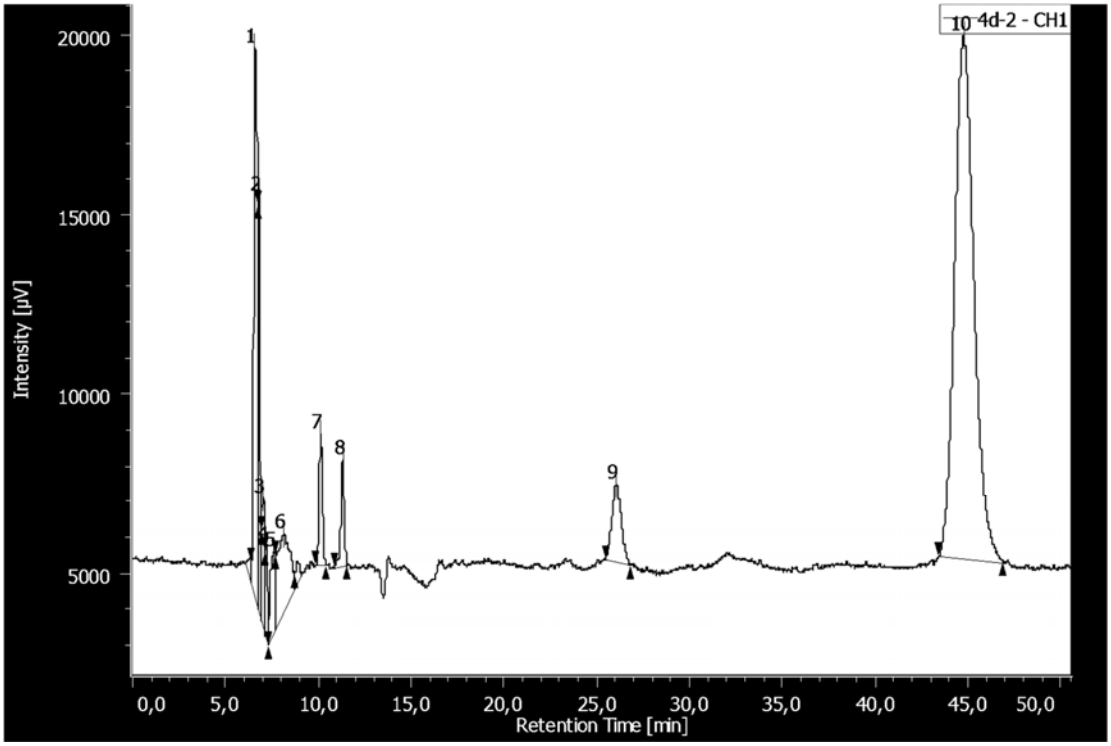

Figure S12. Chiral analysis of (1*R*,4*R*)-4-(1*H*-indol-3-ylmethyl)-1-isopropyl-2*H*-pyrazino[2,1-*b*]quinazolin-3,6-(1*H*, 4*H*)-dione (**4d**). Column: Lux® 5 µm Amylose-1, 250 × 4.6 mm; UV-detection: 254 nm; mobile phase: hexane:ethanol (80:20); flow rate: 0.5 mL/min.

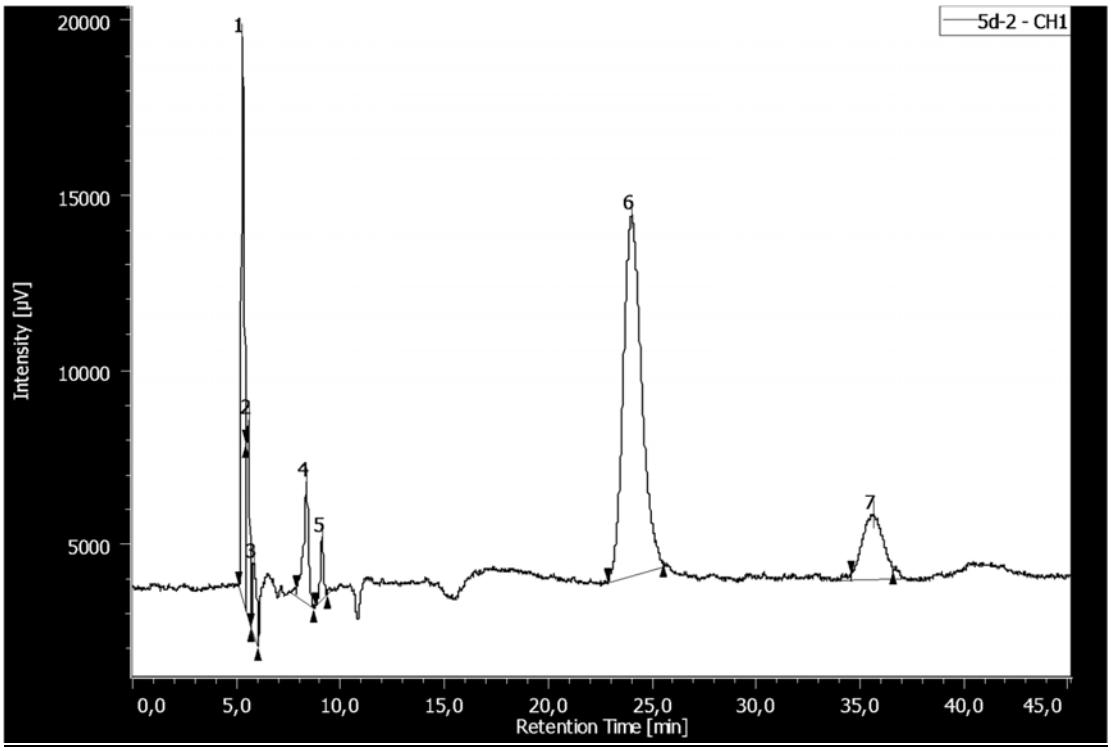

Figure S13. Chiral analysis of (1*S*,4*S*)-4-(1*H*-indol-3-ylmethyl)-1-isobutyl-2*H*-pyrazino[2,1-*b*]quinazolin-3,6-(1*H*, 4*H*)-dione (**5a**). Column: Lux® 5 µm Amylose-1, 250 × 4.6 mm; UV-detection: 254 nm; mobile phase: hexane:ethanol (80:20); flow rate: 0.5 mL/min.

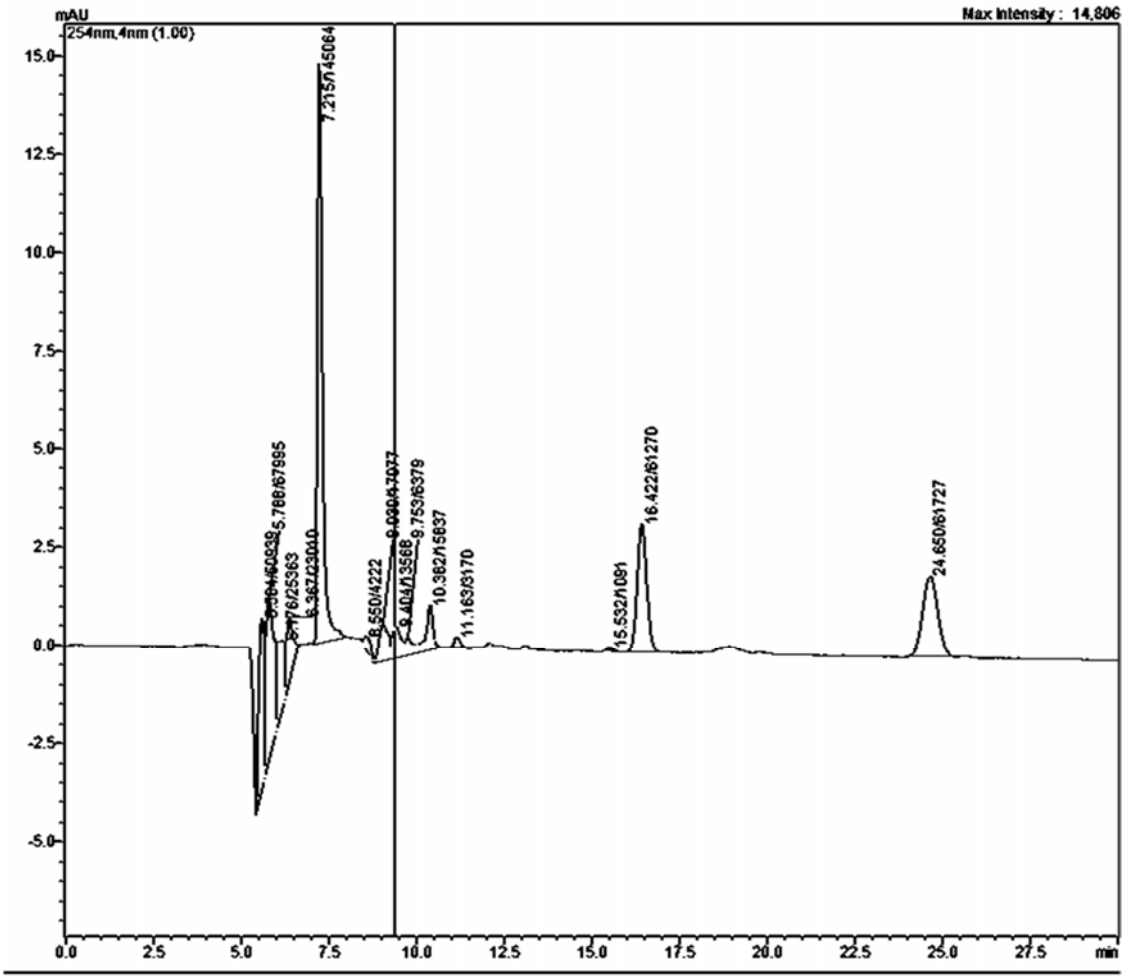

Figure S14. Chiral analysis of (1*S*,4*R*)-4-(1*H*-indol-3-ylmethyl)-1-isobutyl-2*H*-pyrazino[2,1-*b*]quinazolin-3,6-(1*H*, 4*H*)-dione (**5b**). Column: Lux® 5 µm Amylose-1, 250 × 4.6 mm; UV-detection: 254 nm; mobile phase: hexane:ethanol (80:20); flow rate: 0.5 mL/min.

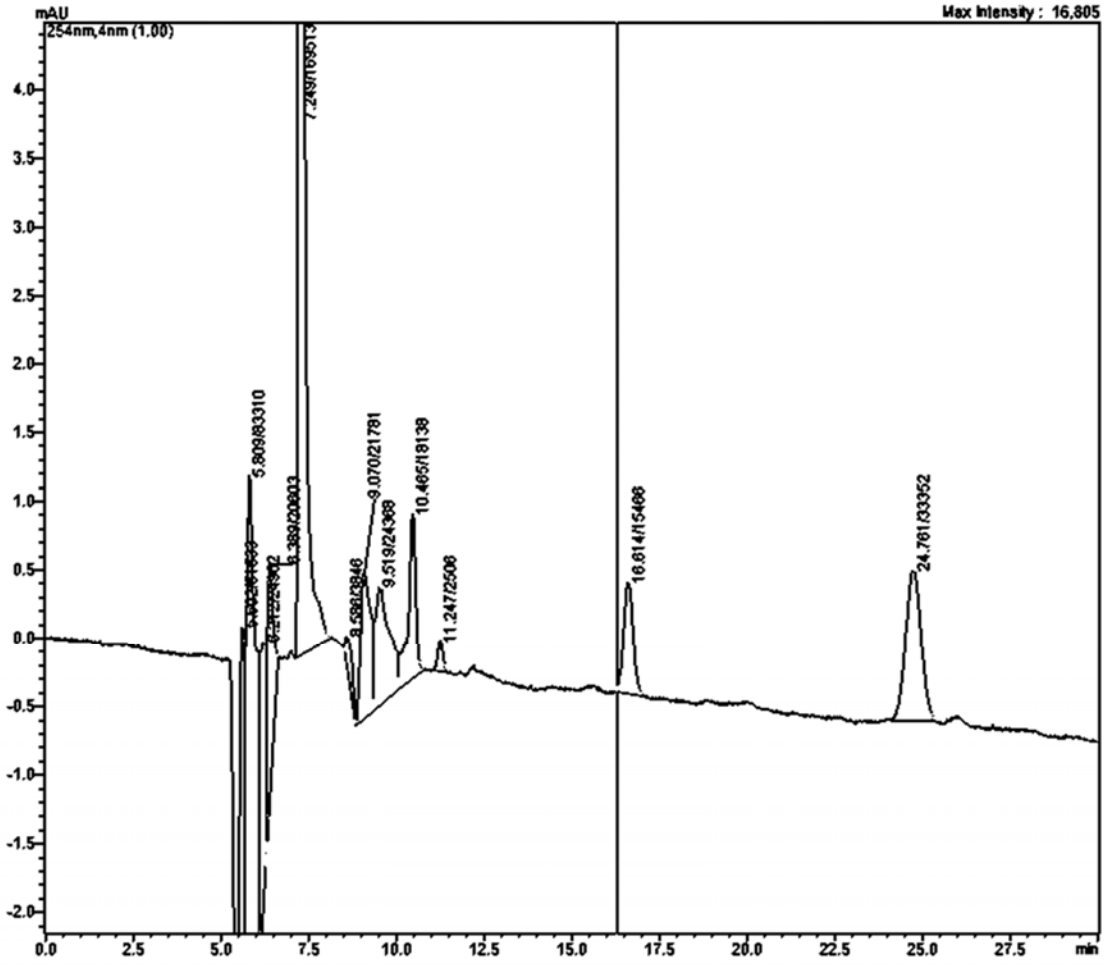

Figure S15. Chiral analysis of (1*R*,4*S*)-4-(1*H*-indol-3-ylmethyl)-1-isobutyl-2*H*-pyrazino[2,1-*b*]quinazolin-3,6-(1*H*, 4*H*)-dione (**5c**). Column: Lux® 5 µm Amylose-1, 250 × 4.6 mm; UV-detection: 254 nm; mobile phase: hexane:ethanol (80:20); flow rate: 0.5 mL/min.

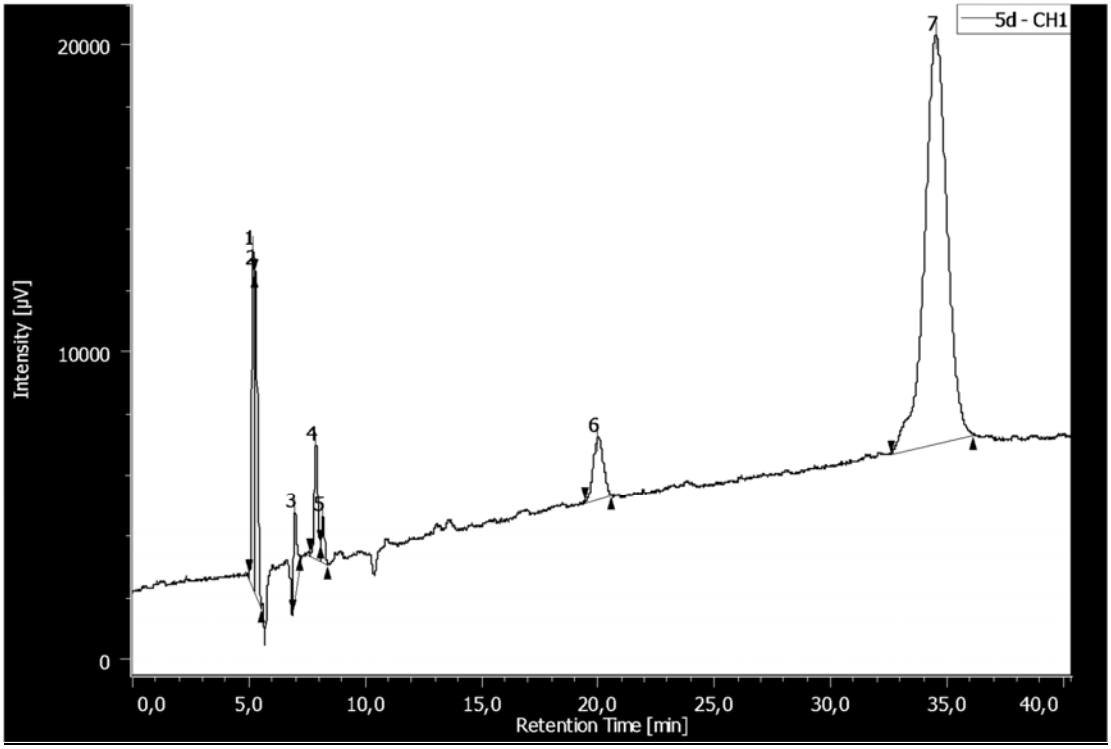

Figure S16. Chiral analysis of (1*R*,4*R*)-4-(1*H*-indol-3-ylmethyl)-1-isobutyl-2*H*-pyrazino[2,1-*b*]quinazolin-3,6-(1*H*, 4*H*)-dione (**5d**). Column: Lux® 5 µm Amylose-1, 250 × 4.6 mm; UV-detection: 254 nm; mobile phase: hexane:ethanol (80:20); flow rate: 0.5 mL/min.

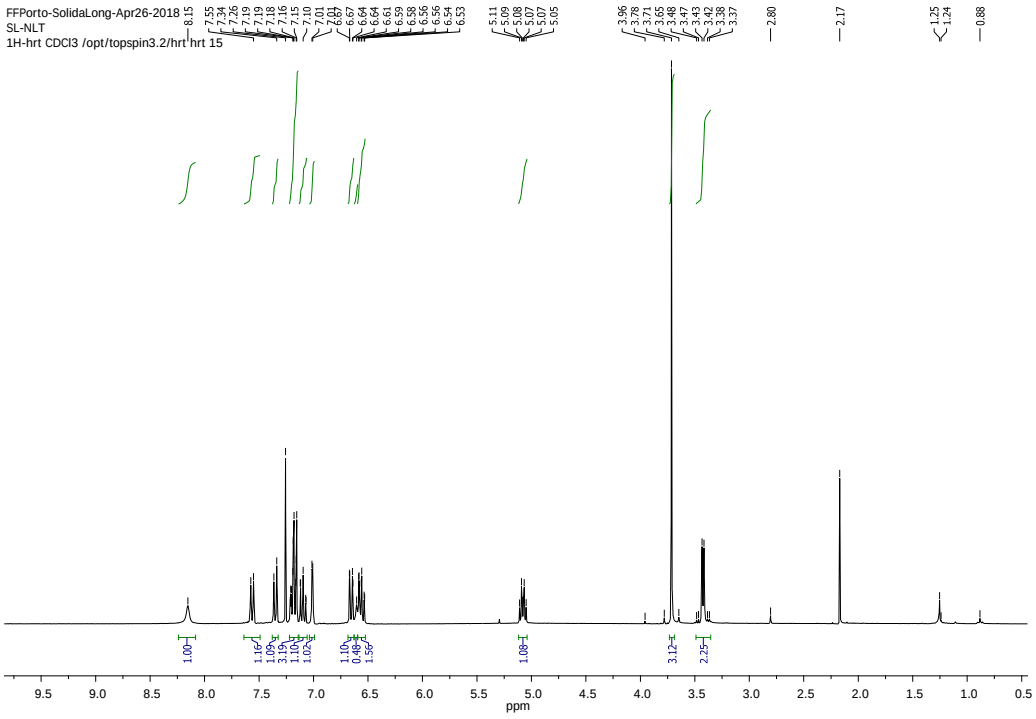

Figure S17. ^{1}H NMR spectrum of *N*-(2-aminobenzoyl)-L-tryptophan methyl ester **(iv-a)** ($CDCl_3$, 300, MHz).

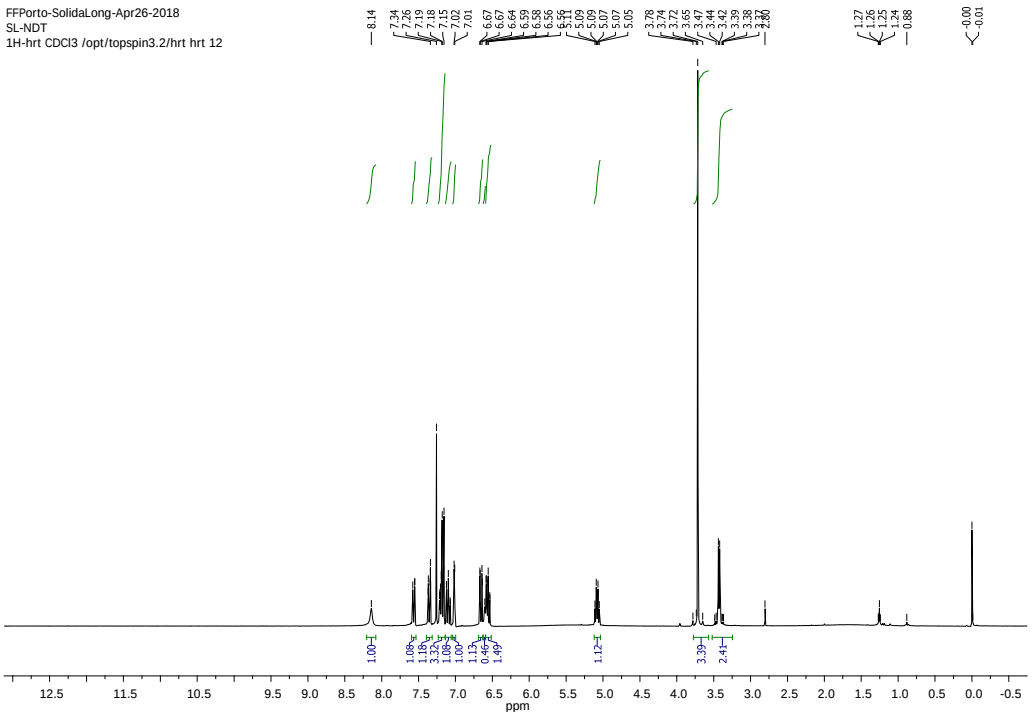

Figure S18. ^{1}H NMR spectrum of *N*-(2-aminobenzoyl)-D-tryptophan methyl ester **(iv-b)** ($CDCl_3$, 300, MHz).

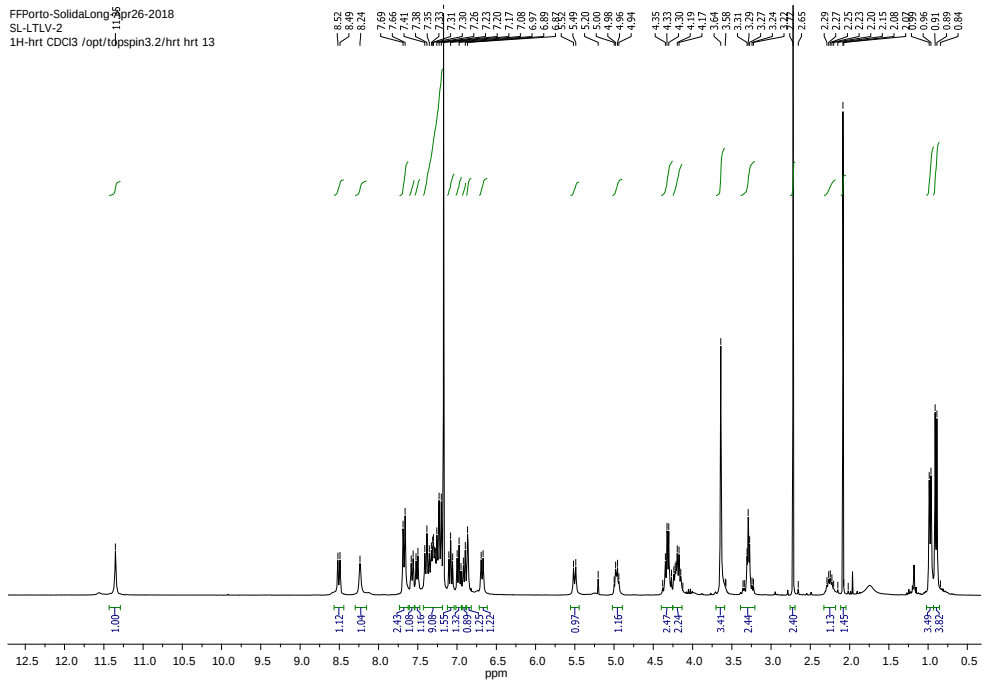

Figure S19. ^{1}H NMR spectrum of *N*-[9*H*-fluoren-9-ylmethoxy)carbonyl]-L-valinyl-2-aminobenzoyl-L-tryptophan methyl ester (**vi-a**) ($CDCl_3$, 300, MHz).

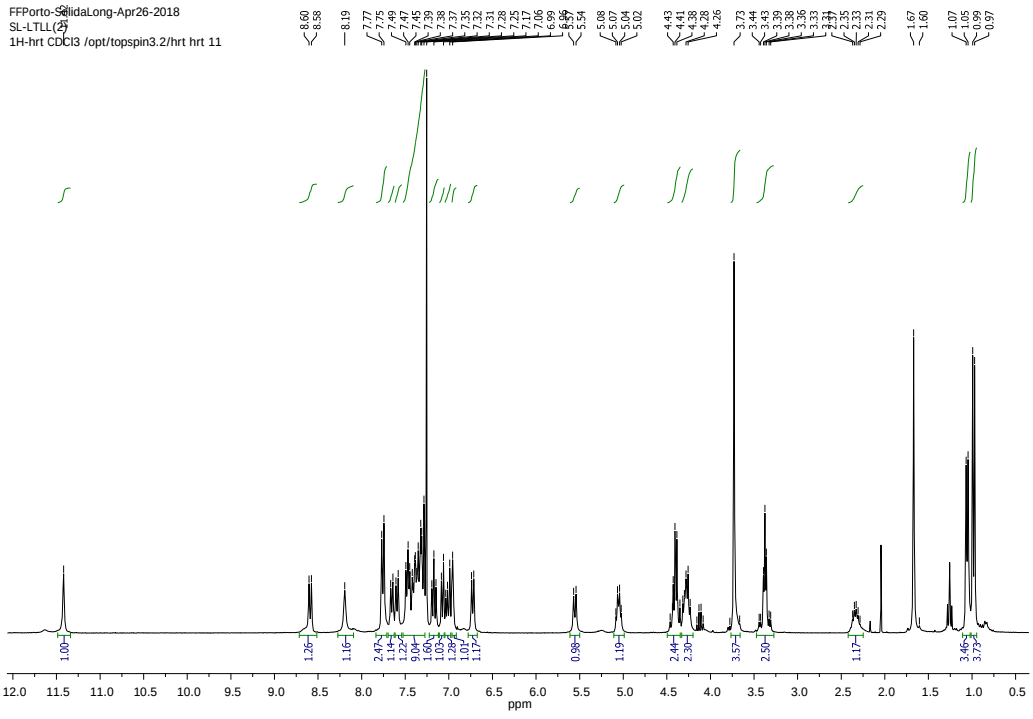

Figure S20. ^{1}H NMR spectrum of *N*-[9*H*-fluoren-9-ylmethoxy)carbonyl]-L-methylpentanyl-2*H*-aminobenzoyl-L- tryptophan methyl ester (**vi-b**) ($CDCl_3$, 300, MHz).

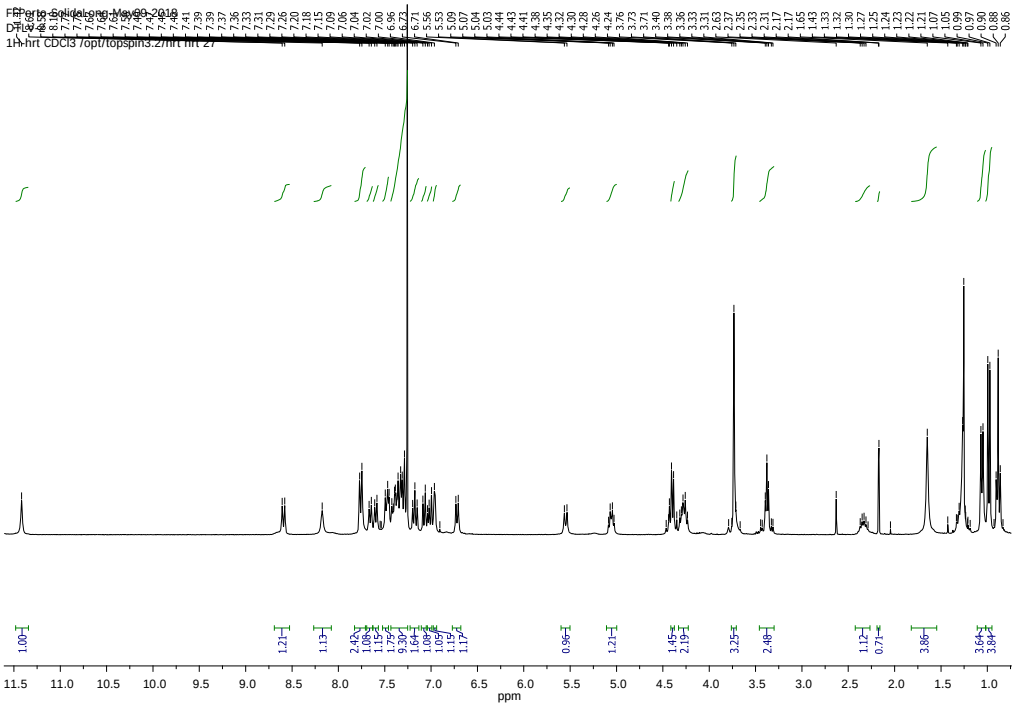

Figure S21. ^{1}H NMR spectrum of *N*-[9*H*-fluoren-9-ylmethoxy)carbonyl]-D-valinyl-2-aminobenzoyl-D-tryptophan methyl ester (**vi-c**) ($CDCl_3$, 300, MHz).

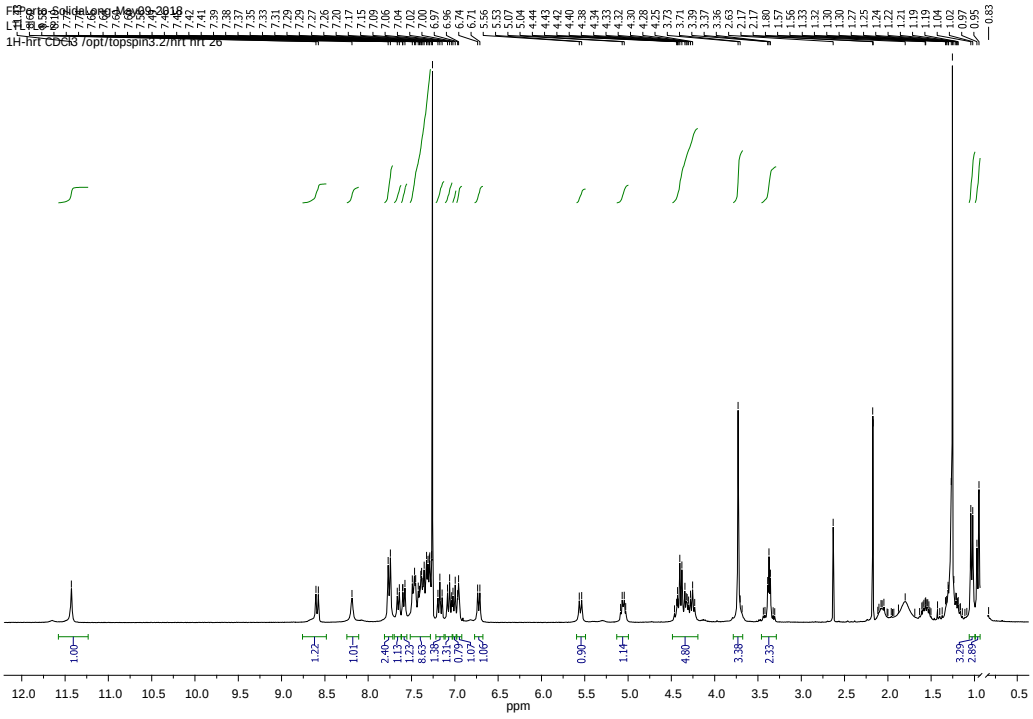

Figure S22. ^{1}H NMR spectrum of *N*-[9*H*-fluoren-9-ylmethoxy)carbonyl]-D-methylpentyl-2-aminobenzoyl-D- tryptophan methyl ester (**vi-d**) ($CDCl_3$, 300, MHz).

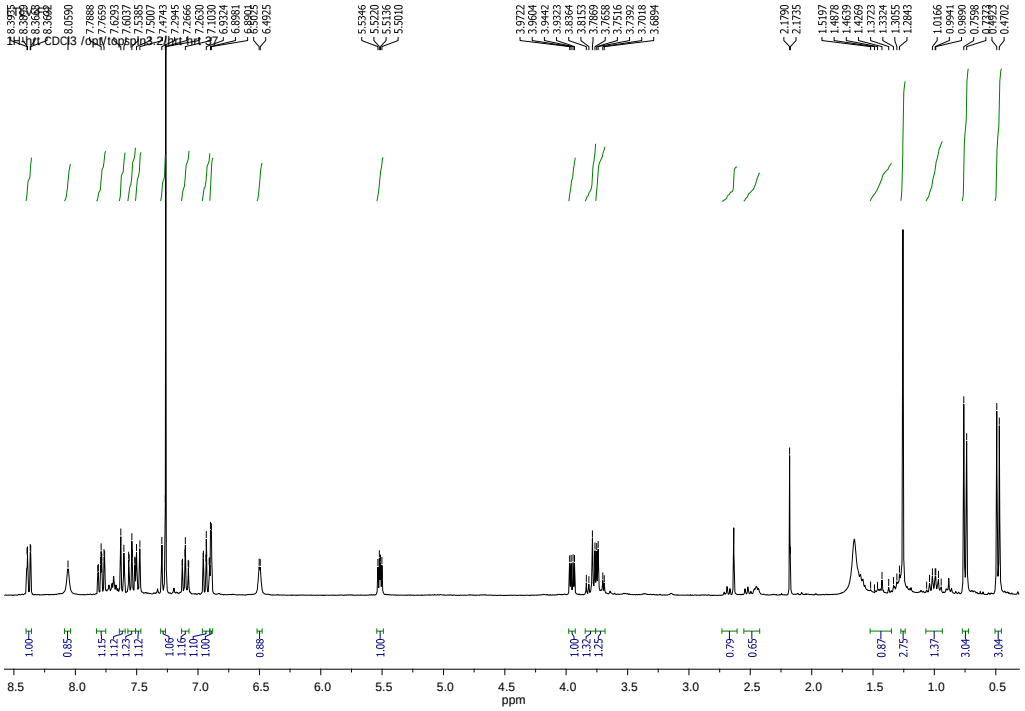

Figure S23. ^{1}H NMR spectrum of (1*S*,4*S*)-4-(1*H*-indol-3-ylmethyl)-1-isopropyl-2*H*-pyrazino[2,1-*b*]quinazolin-3,6-(1*H*, 4*H*)-dione (**4a**) (CDCl$_3$, 300, MHz).

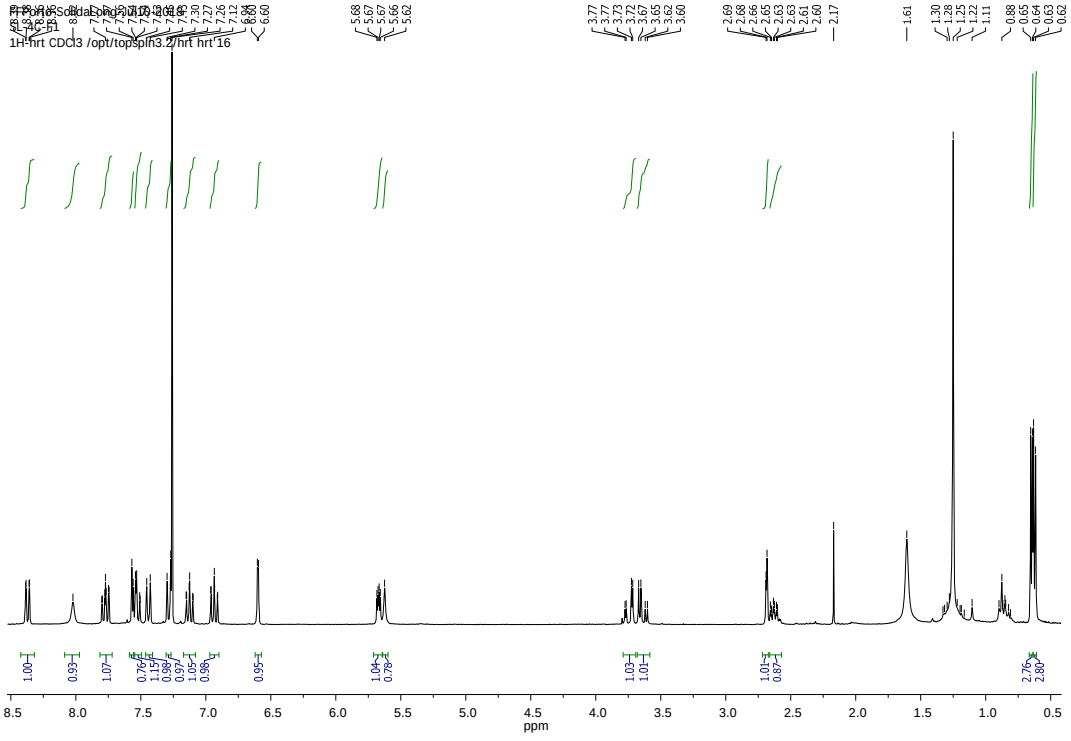

Figure S24. ^{1}H NMR spectrum of (1*R*,4*S*)-4-(1*H*-Indol-3-ylmethyl)-1-isopropyl-2*H*-pyrazino[2,1-*b*]quinazoline-3,6-(1*H*,4*H*)-dione (**4b**) (CDCl$_3$, 300, MHz).

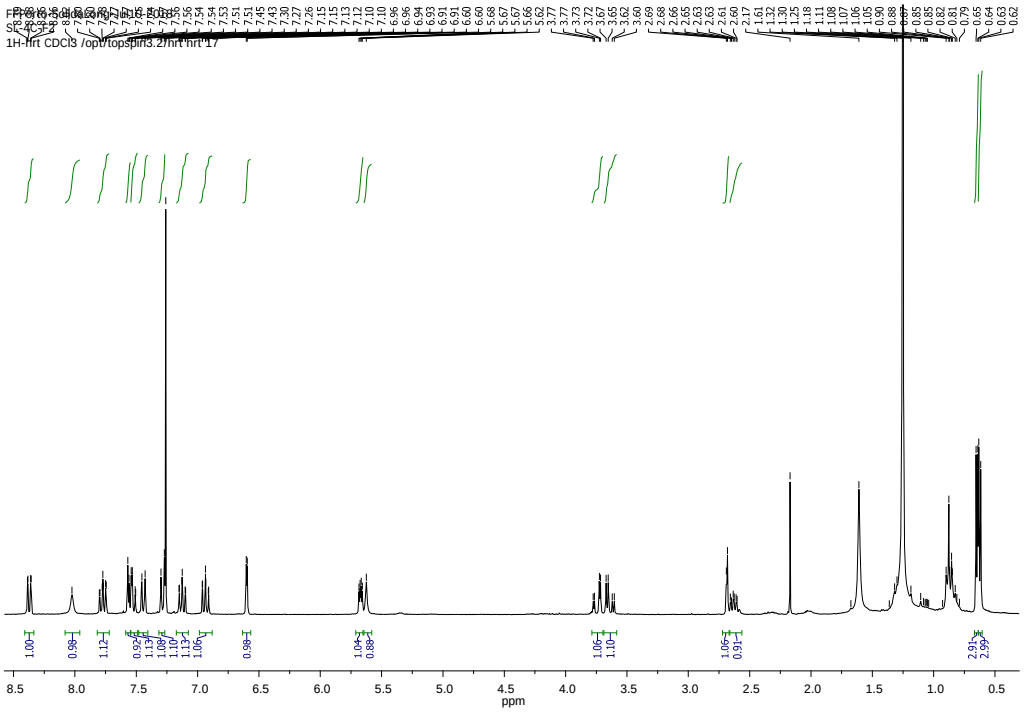

Figure S25. ^{1}H NMR spectrum of (1*S*,4*R*)-4-(1*H*-Indol-3-ylmethyl)-1-isopropyl-2*H*-pyrazino[2,1-*b*]quinazoline-3,6-(1*H*,4*H*)-dione (**4c**) ($CDCl_3$, 300, MHz).

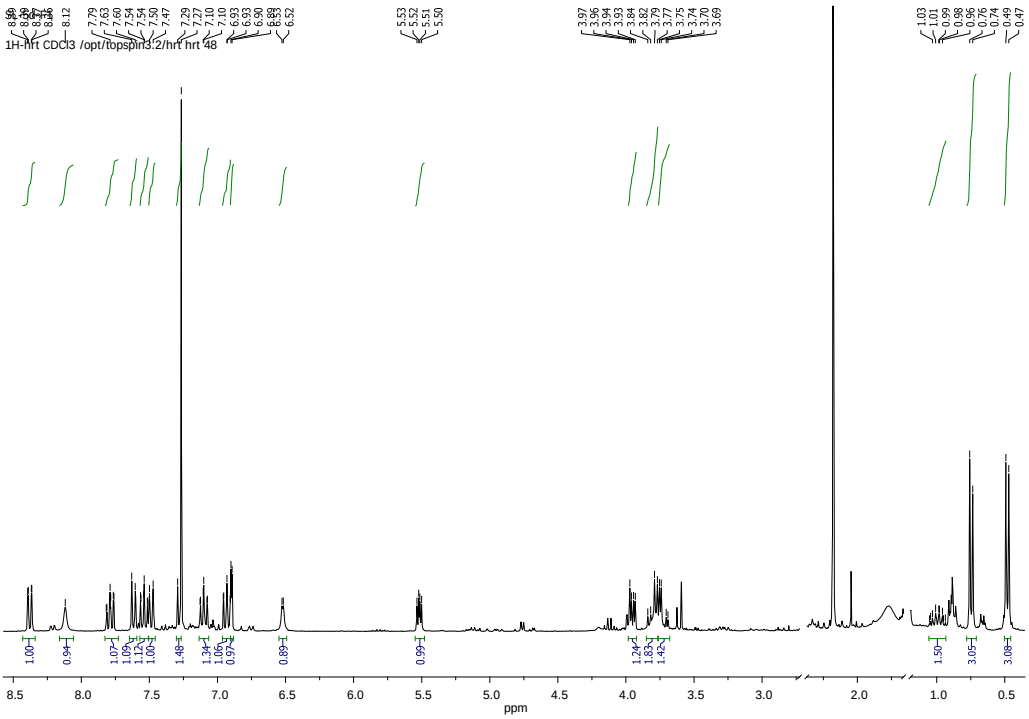

Figure S26. ^{1}H NMR spectrum of (1*R*,4*R*)-4-(1*H*-indol-3-ylmethyl)-1-isopropyl-2*H*-pyrazino[2,1-*b*]quinazolin-3,6-(1*H*, 4*H*)-dione (**4d**) ($CDCl_3$, 300, MHz).

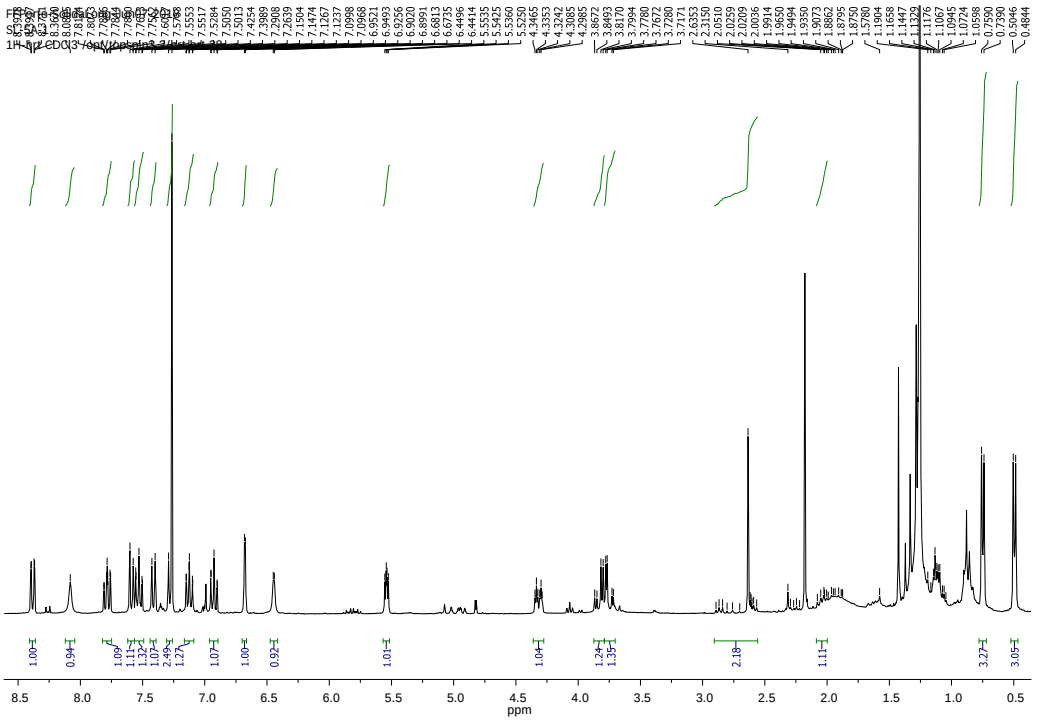

Figure S27. ^{1}H NMR spectrum of (1*S*,4*S*)-4-(1*H*-indol-3-ylmethyl)-1-isobutyl-2*H*-pyrazino[2,1-*b*]quinazolin-3,6-(1*H*, 4*H*)-dione (**5a**) ($CDCl_3$, 300, MHz).

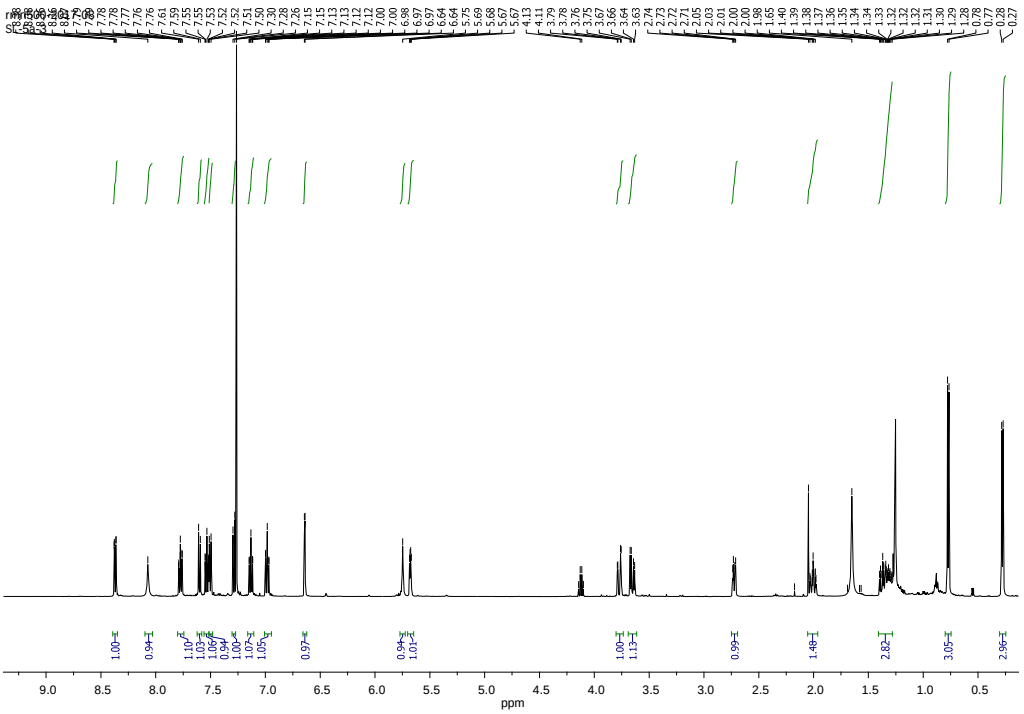

Figure S28. ^{1}H NMR spectrum of (1*R*,4*S*)-4-(1*H*-Indol-3-ylmethyl)-1-isobutyl-2*H*-pyrazino[2,1-*b*]quinazoline-3,6-(1*H*,4*H*)-dione (**5b**) ($CDCl_3$, 300, MHz).

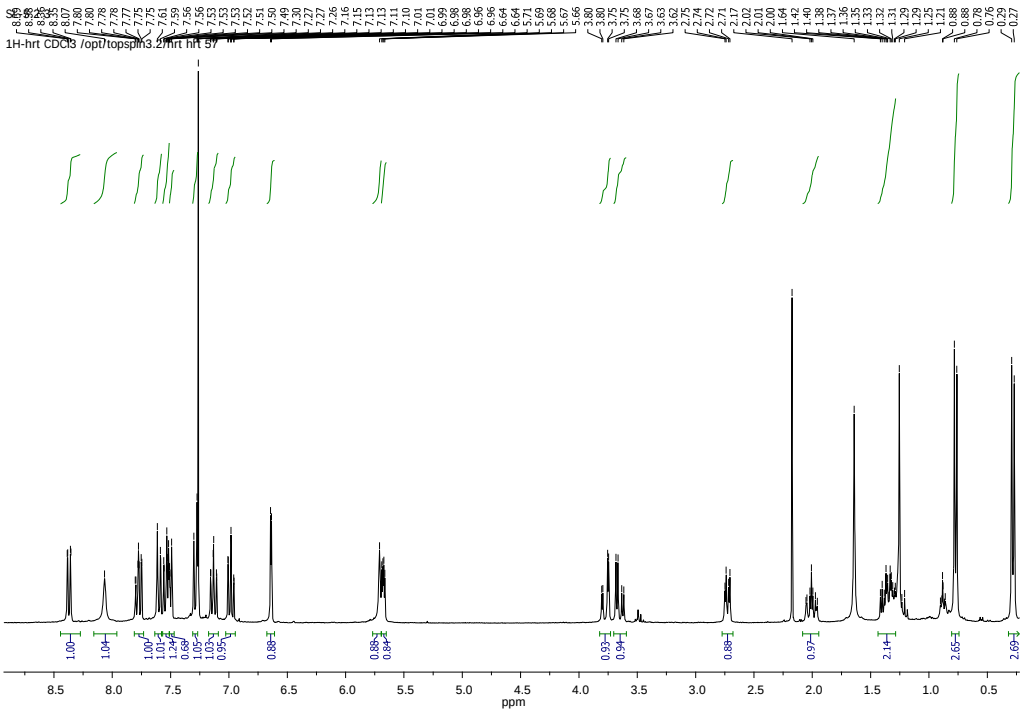

Figure S29. ^{1}H NMR spectrum of (1*S*,4*R*)-4-(1*H*-Indol-3-ylmethyl)-1-isobutyl-2*H*-pyrazino[2,1-*b*]quinazoline-3,6-(1*H*,4*H*)-dione (**5c**) ($CDCl_3$, 300, MHz).

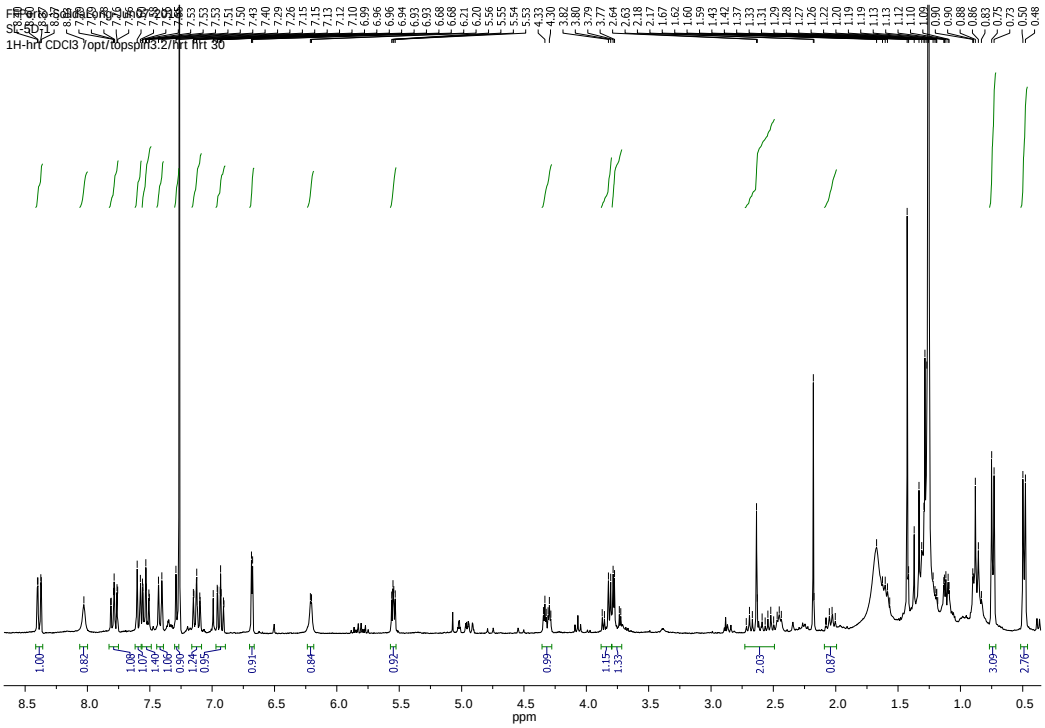

Figure S30. ^{1}H NMR spectrum of (1*R*,4*R*)-4-(1*H*-indol-3-ylmethyl)-1-isobutyl-2*H*-pyrazino[2,1-*b*]quinazolin-3,6-(1*H*, 4*H*)-dione (**5d**) (CDCl$_3$, 300, MHz).

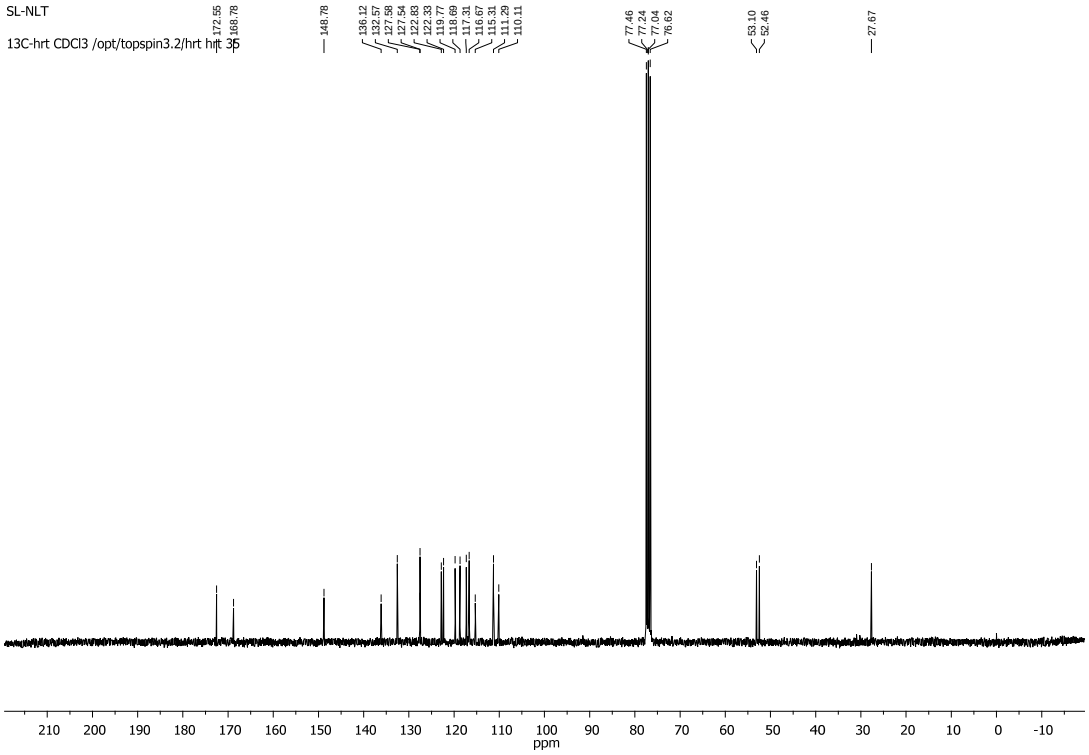

Figure S31. ^{13}C NMR spectrum of *N*-(2-aminobenzoyl)-L-tryptophan methyl ester **(iv-a)** (CDCl$_3$, 75, MHz).

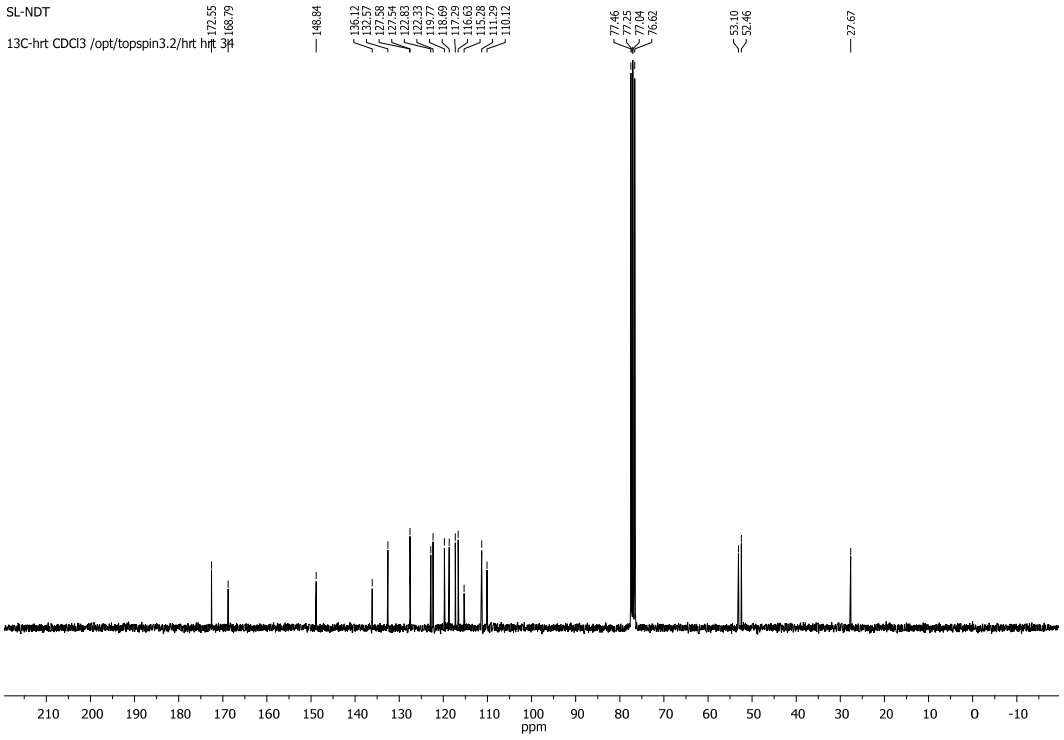

Figure S32. ^{13}C NMR spectrum of *N*-(2-aminobenzoyl)-D-tryptophan methyl ester **(iv-b)** ($CDCl_3$, 75, MHz).

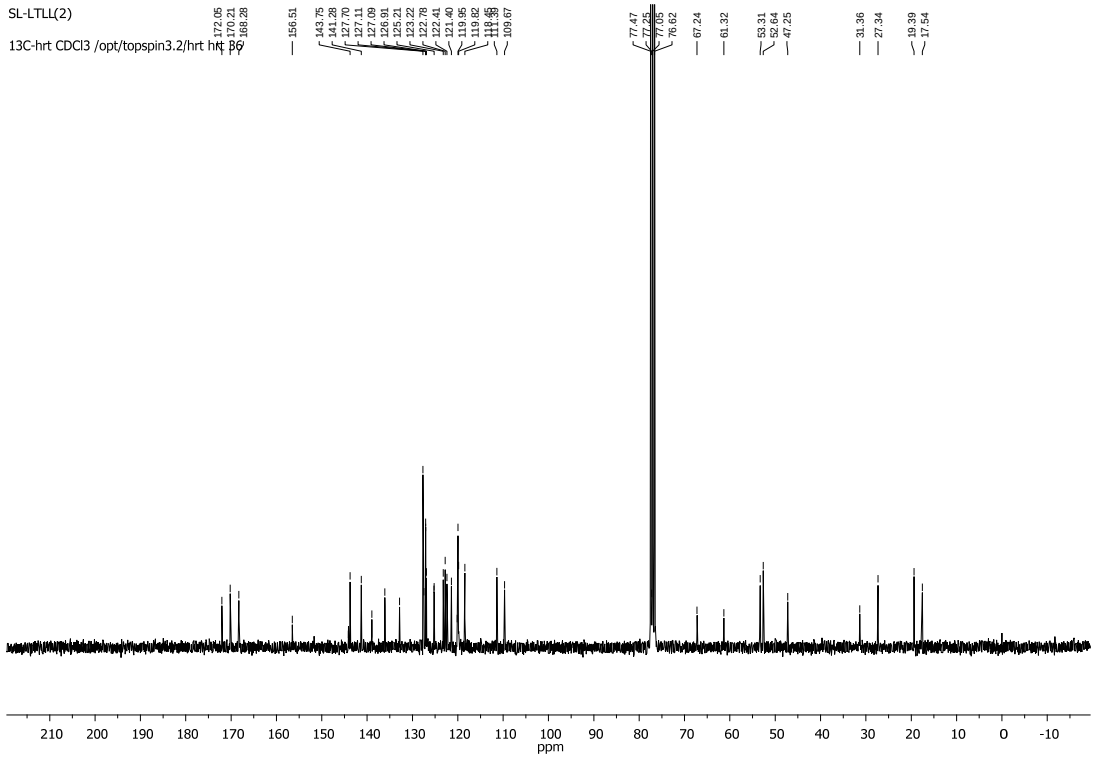

Figure S33. ^{13}C NMR spectrum of *N*-[9*H*-fluoren-9-ylmethoxy)carbonyl]-L-valinyl-2-aminobenzoyl-L-tryptophan methyl ester (**vi-a**) ($CDCl_3$, 75, MHz).

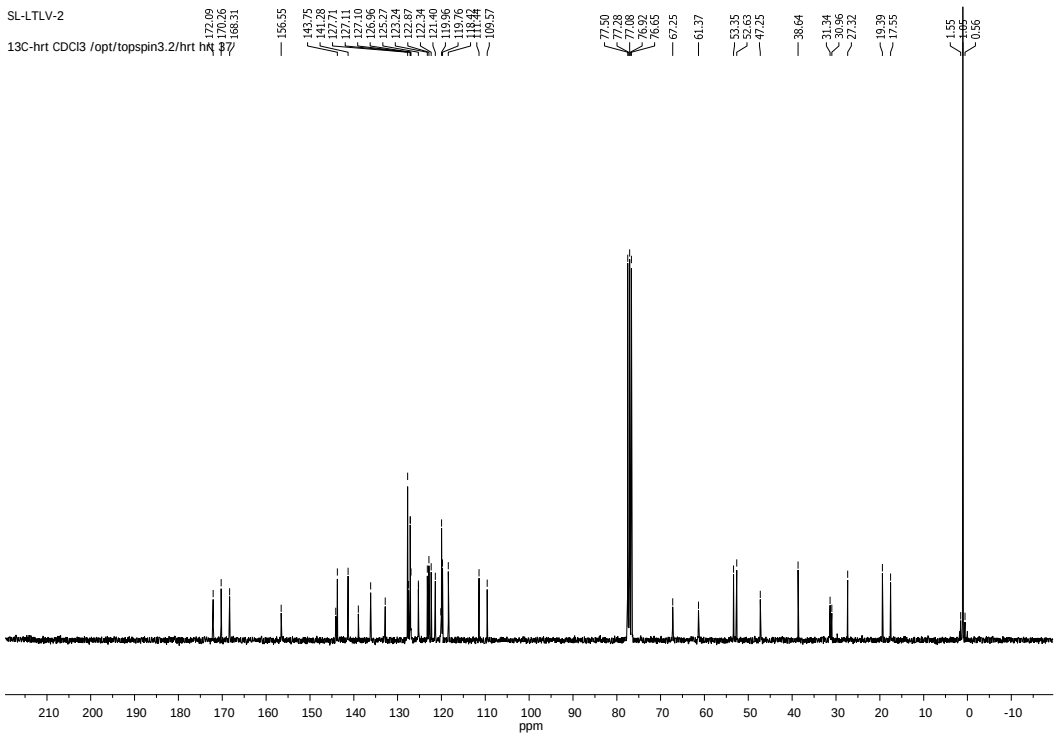

Figure S34. ^{13}C NMR spectrum of *N*-[9*H*-fluoren-9-ylmethoxy)carbonyl]-L-methylpentanyl-2*H*-aminobenzoyl-L- tryptophan methyl ester (**vi-b**) ($CDCl_3$, 75, MHz).

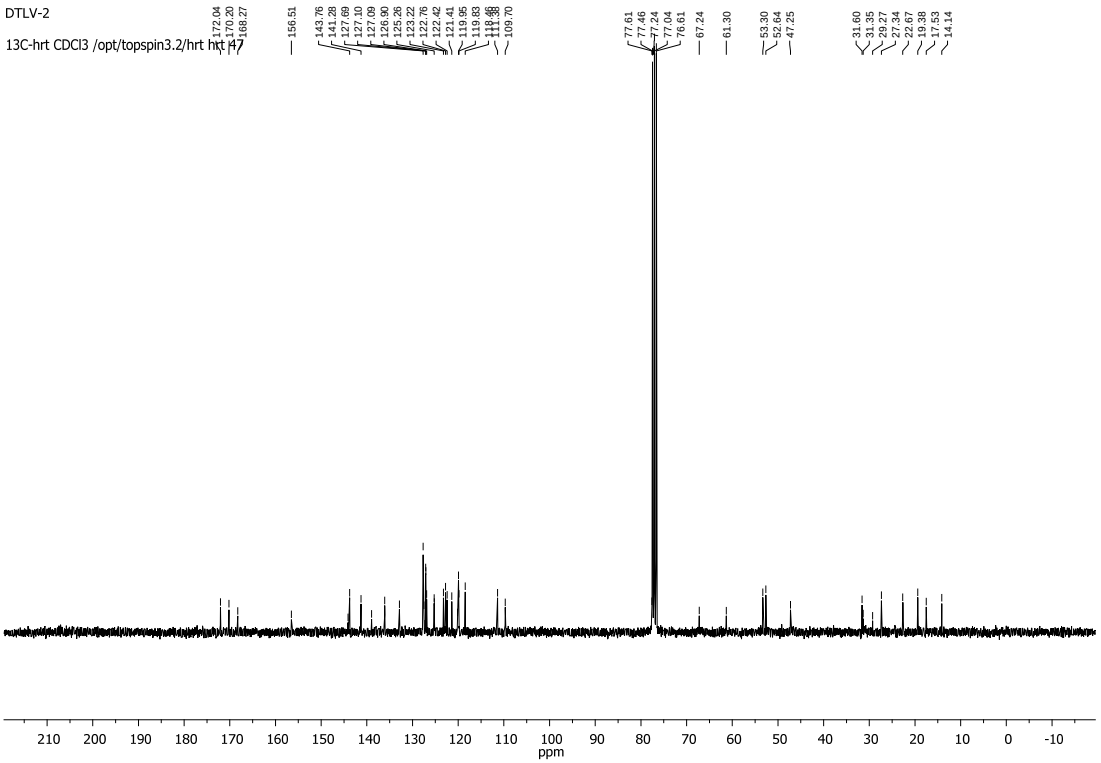

Figure S35. ^{13}C NMR spectrum of *N*-[9*H*-fluoren-9-ylmethoxy)carbonyl]-D-valinyl-2-aminobenzoyl-D-tryptophan methyl ester (**vi-c**) ($CDCl_3$, 75, MHz).

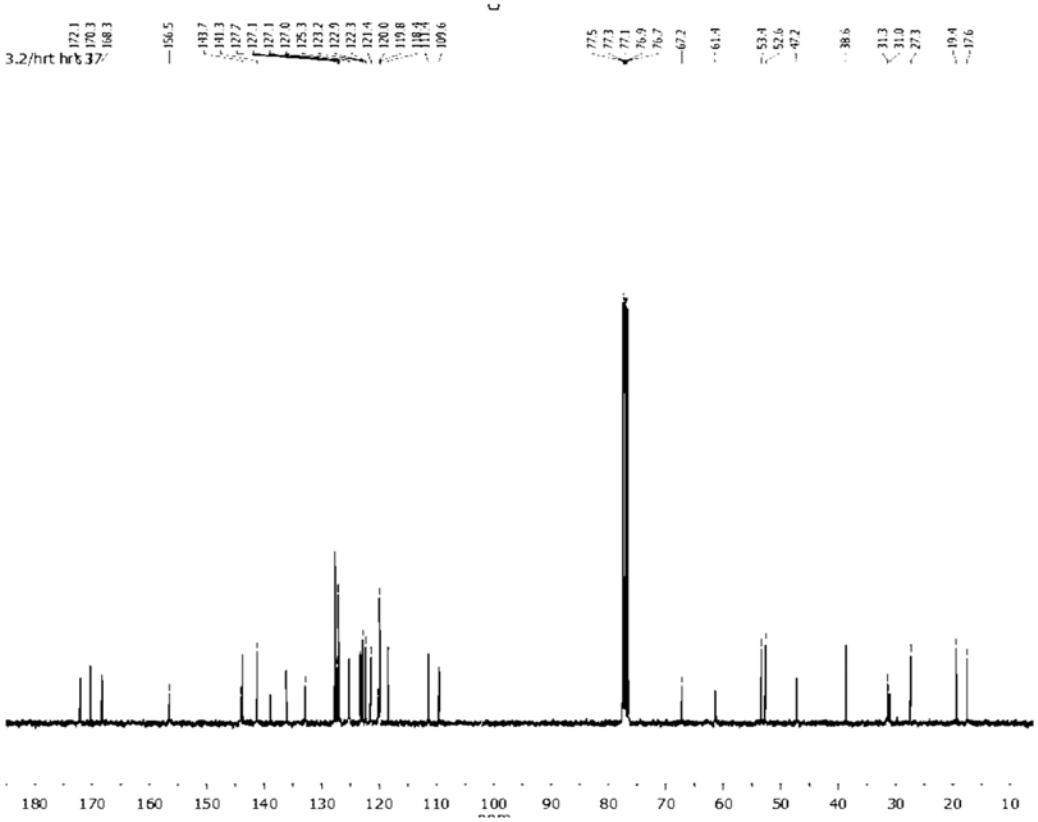

Figure S36. ^{13}C NMR spectrum of *N*-[9*H*-fluoren-9-ylmethoxy)carbonyl]-D-methylpentyl-2-aminobenzoyl-D- tryptophan methyl ester (**vi-d**) ($CDCl_3$, 75, MHz).

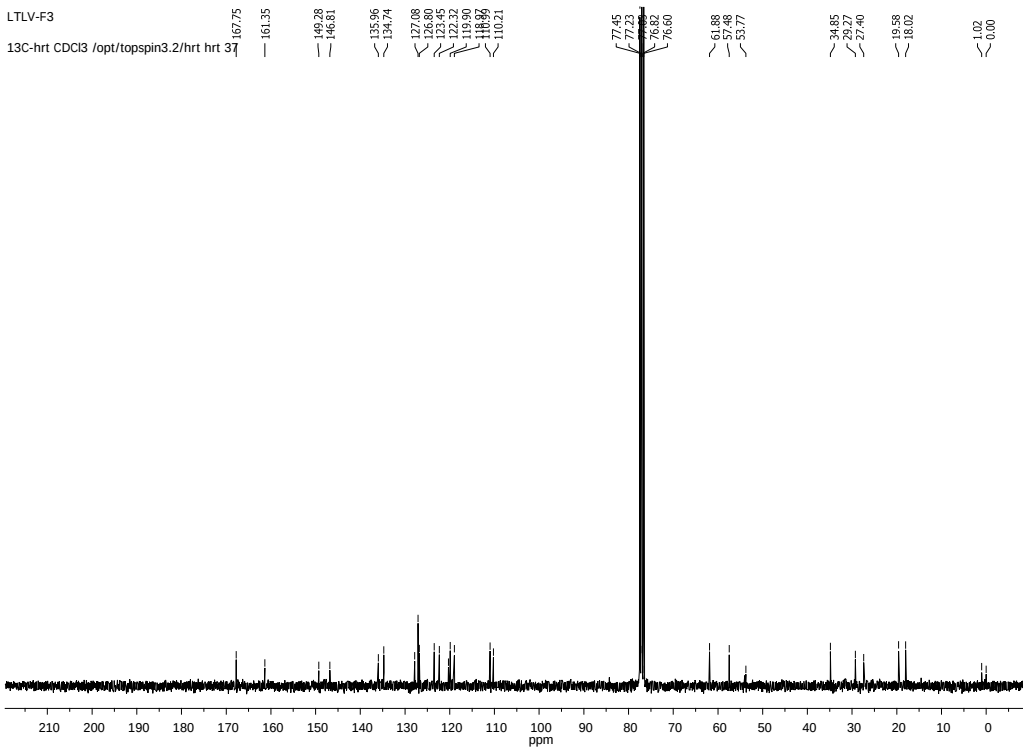

Figure S37. ^{13}C NMR spectrum of (1*S*,4*S*)-4-(1*H*-indol-3-ylmethyl)-1-isopropyl-2*H*-pyrazino[2,1-*b*]quinazolin-3,6-(1*H*, 4*H*)-dione (**4a**) ($CDCl_3$, 75, MHz).

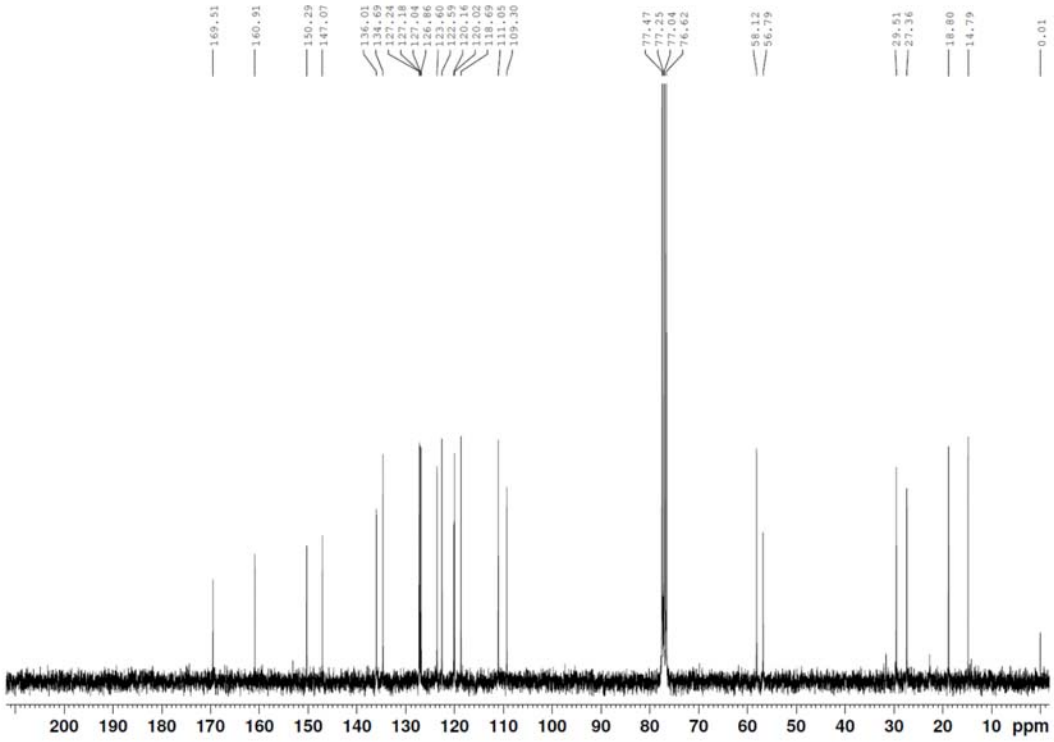

Figure S38. ^{13}C NMR spectrum of (1*R*,4*S*)-4-(1*H*-Indol-3-ylmethyl)-1-isopropyl-2*H*-pyrazino[2,1-*b*]quinazoline-3,6-(1*H*,4*H*)-dione (**4b**) ($CDCl_3$, 75, MHz).

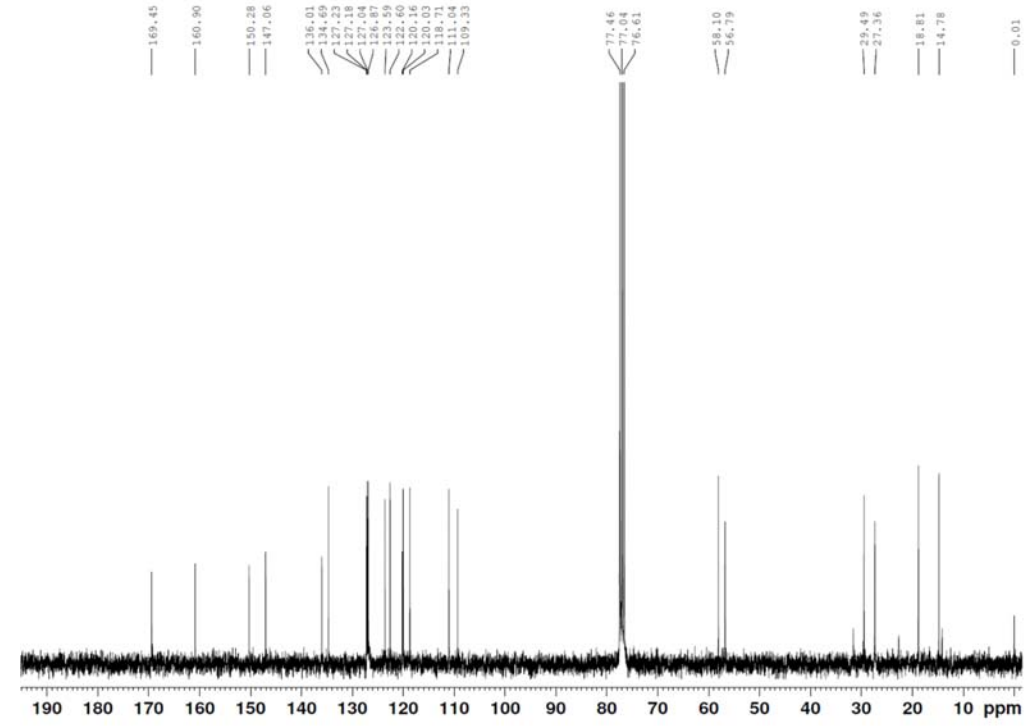

Figure S39. ^{13}C NMR spectrum of (1*S*,4*R*)-4-(1*H*-Indol-3-ylmethyl)-1-isopropyl-2*H*-pyrazino[2,1-*b*]quinazoline-3,6-(1*H*,4*H*)-dione (**4c**) ($CDCl_3$, 75, MHz).

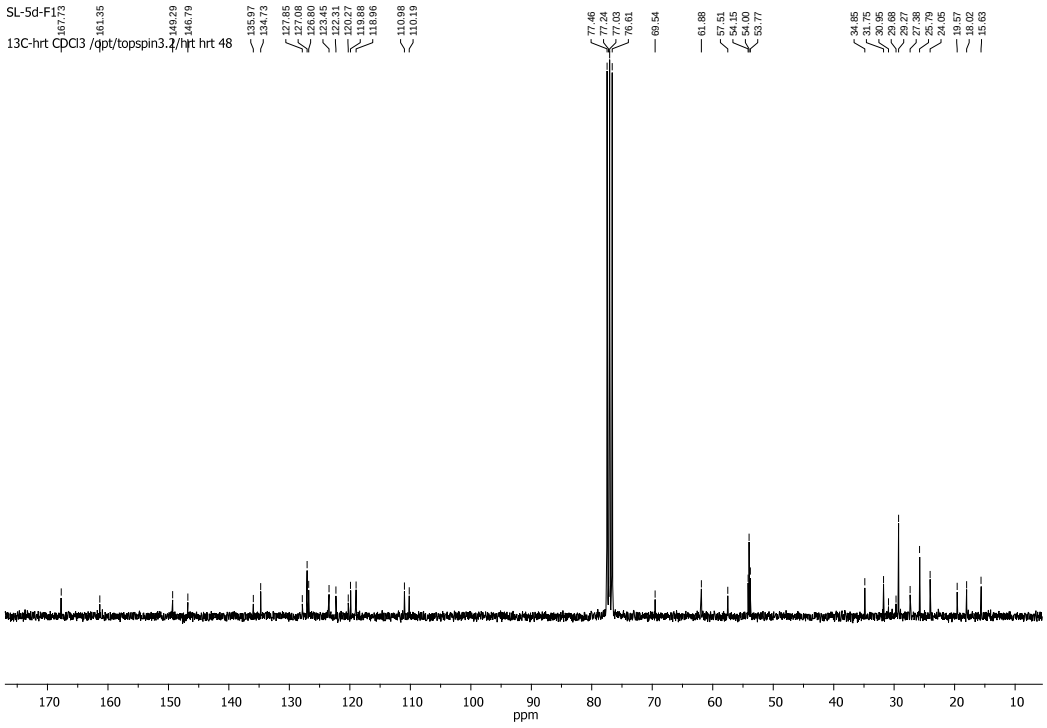

Figure S40. ^{13}C NMR spectrum of (1*R*,4*R*)-4-(1*H*-indol-3-ylmethyl)-1-isopropyl-2*H*-pyrazino[2,1-*b*]quinazolin-3,6-(1*H*, 4*H*)-dione (**4d**) ($CDCl_3$, 75, MHz).

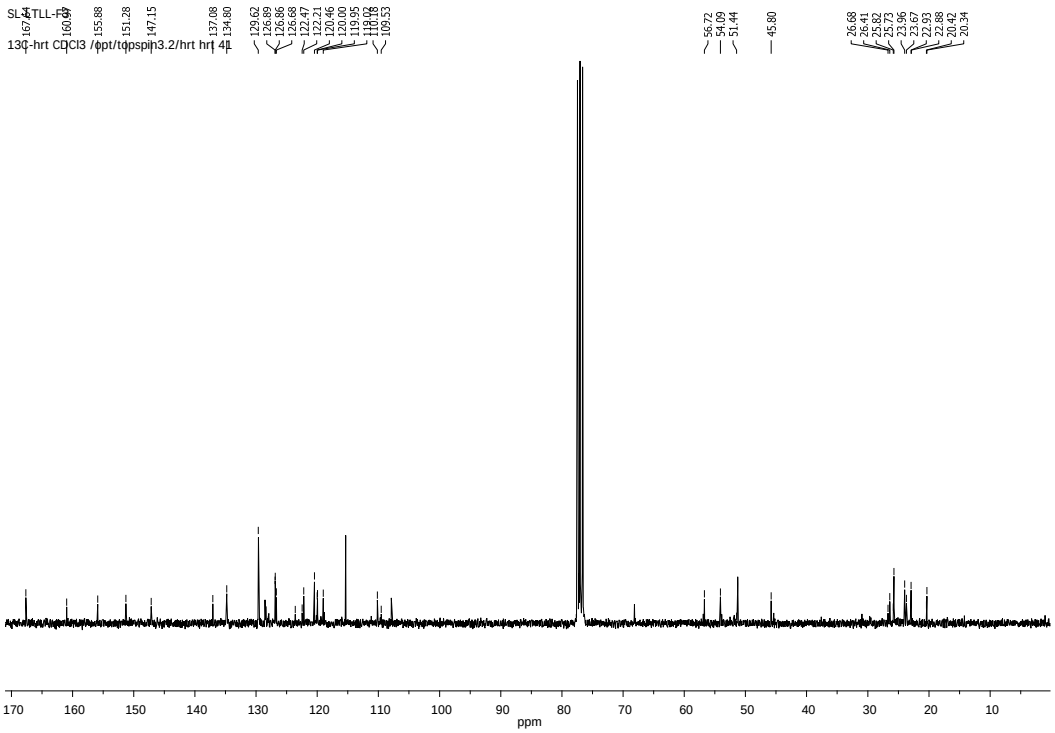

Figure S41. ^{13}C NMR spectrum of (1*S*,4*S*)-4-(1*H*-indol-3-ylmethyl)-1-isobutyl-2*H*-pyrazino[2,1-*b*]quinazolin-3,6-(1*H*, 4*H*)-dione (**5a**) ($CDCl_3$, 75, MHz).

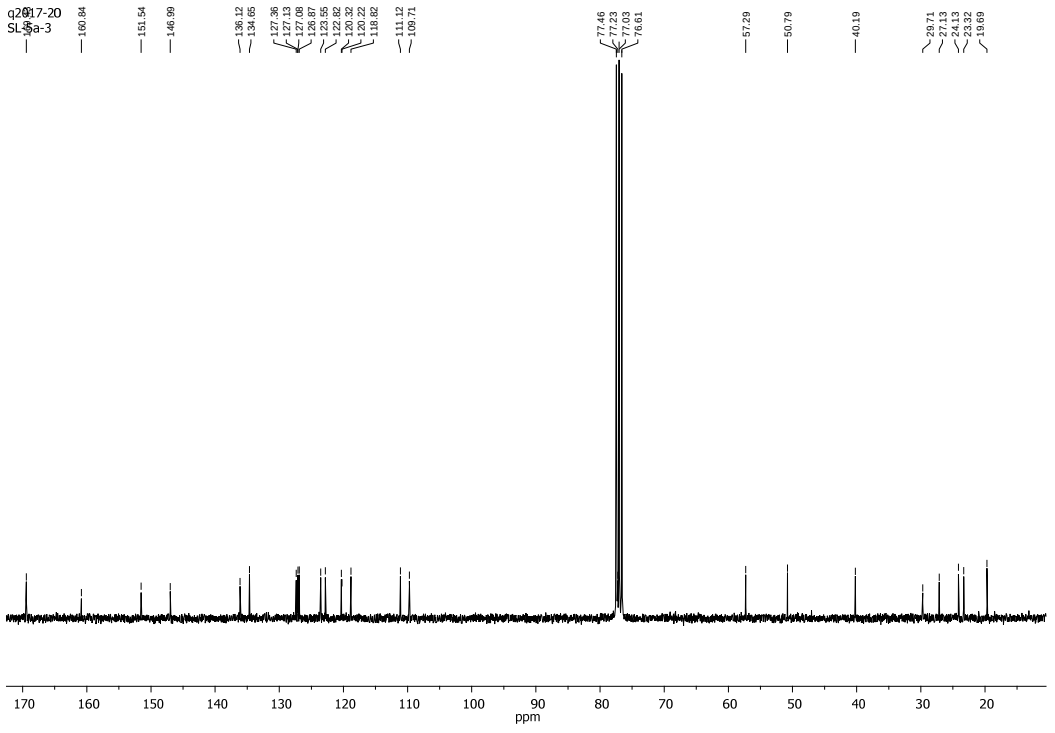

Figure S42. ^{13}C NMR spectrum of (1*R*,4*S*)-4-(1*H*-Indol-3-ylmethyl)-1-isobutyl-2*H*-pyrazino[2,1-*b*]quinazoline-3,6-(1*H*,4*H*)-dione (**5b**) ($CDCl_3$, 75, MHz)

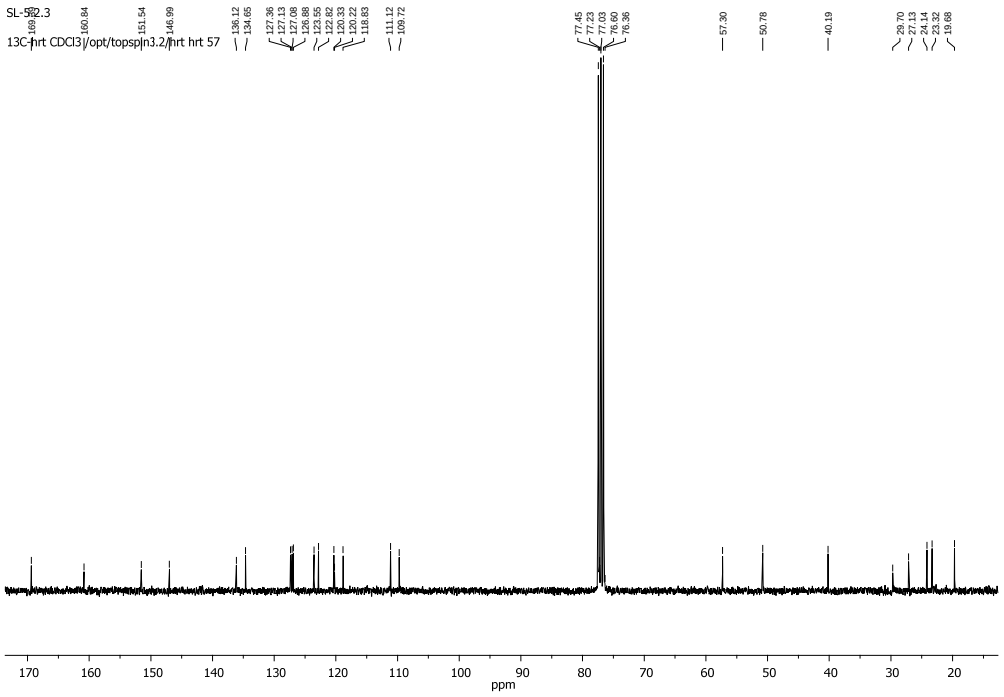

Figure S43. [1]C NMR spectrum of (1*S*,4*R*)-4-(1*H*-Indol-3-ylmethyl)-1-isobutyl-2*H*-pyrazino[2,1-*b*]quinazoline-3,6-(1*H*,4*H*)-dione (**5c**) ($CDCl_3$, 75, MHz).

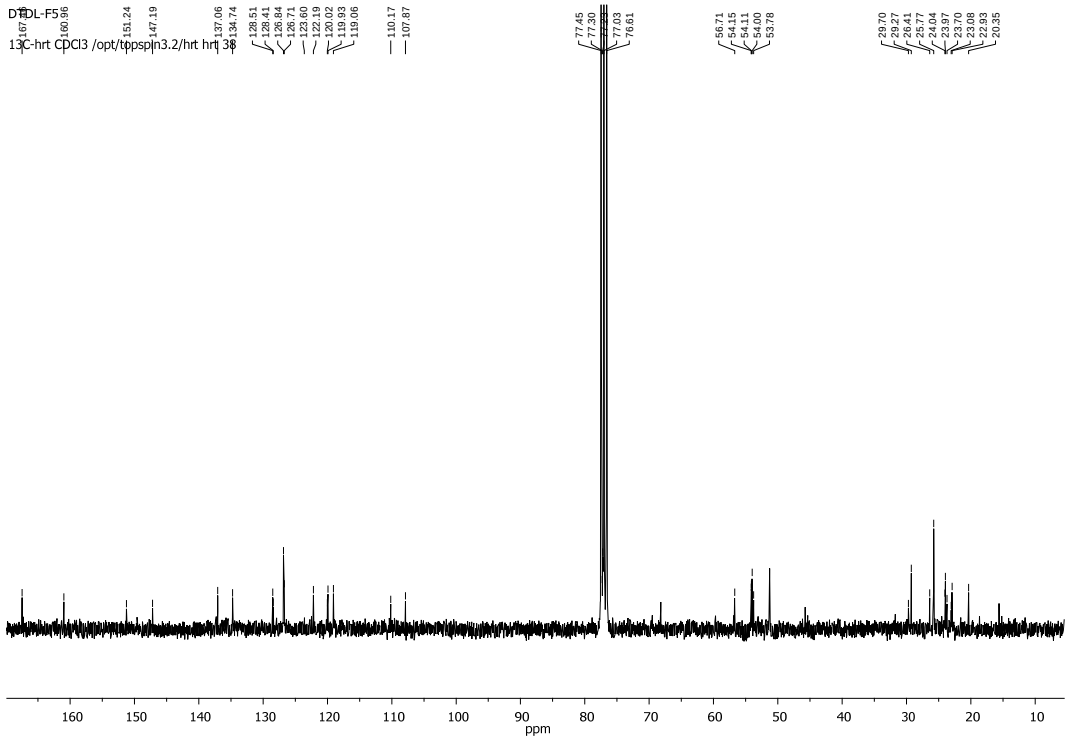

Figure S44. [13]C NMR spectrum of (1*R*,4*R*)-4-(1*H*-indol-3-ylmethyl)-1-isobutyl-2*H*-pyrazino[2,1-*b*]quinazolin-3,6-(1*H*, 4*H*)-dione (**5d**) ($CDCl_3$, 75, MHz).

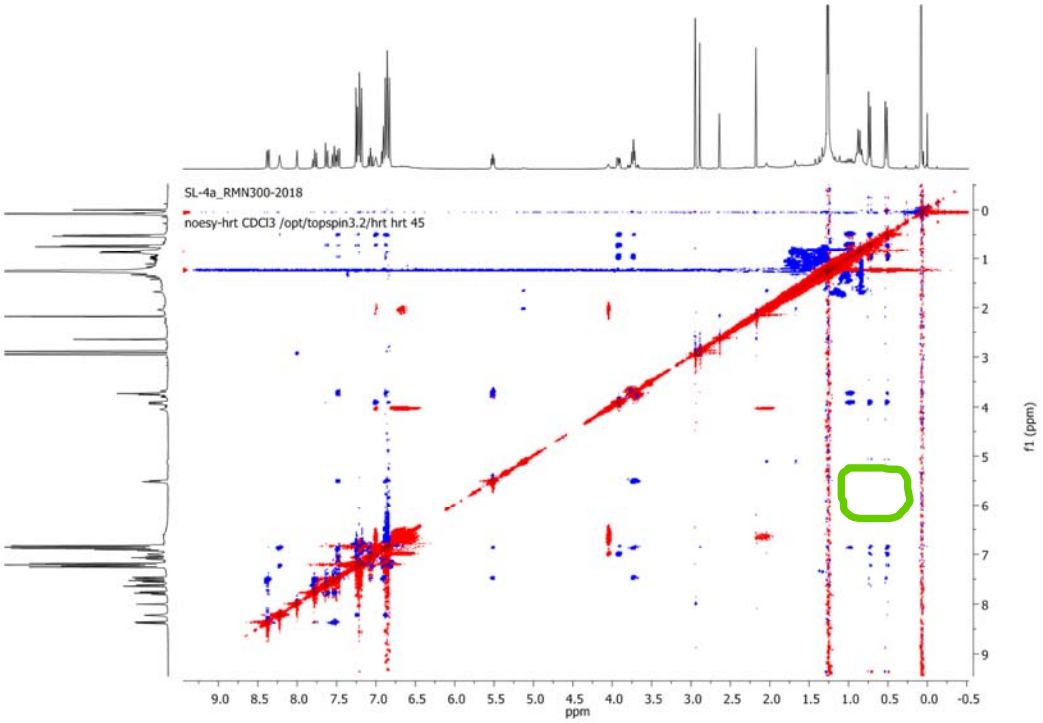

Figure S45. NOESY spectrum of (1*S*,4*R*)-4-(1*H*-Indol-3-ylmethyl)-1-isopropyl-2*H*-pyrazino[2,1-*b*]quinazoline-3,6-(1*H*,4*H*)-dione (**4c**) ($CDCl_3$, 300, MHz). The green circle represents no correlation of proton of C-1′ methyl group and H-4.

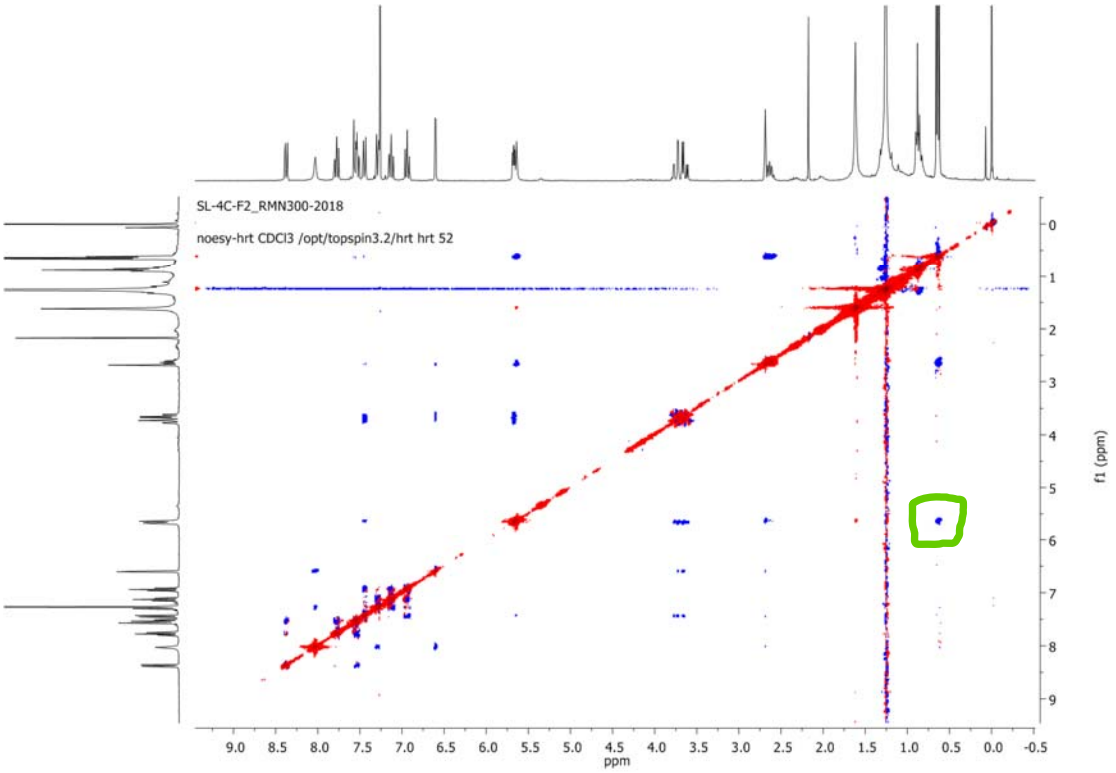

Figure S46. NOESY spectrum of (1*S*,4*S*)-4-(1*H*-Indol-3-ylmethyl)-1-isopropyl-2*H*-pyrazino[2,1-*b*]quinazoline-3,6-(1*H*,4*H*)-dione (**4a**) ($CDCl_3$, 300, MHz). The green circle represents the correlation of proton of C-1′ methyl group and H-4